R E

Form Approved
OMB No. 0704-0188

1. AGENCY USE ONLY (Leave blank)	2. REPORT DATE	3. REPORT TYPE AND DATES COVERED
	27 June 1994	Summary 01 Oct 93 - 31 May 94

4. TITLE AND SUBTITLE

Thermo-fluid mechanic study of thermoacoustic devices

5. FUNDING NUMBERS

PE 61153N
G N0001494J0063
TA 3126971

6. AUTHOR(S)

A. Prosperetti, C. Herman, O. Knio

7. PERFORMING ORGANIZATION NAME(S) AND ADDRESS(ES)

The Johns Hopkins University
Department of Mechanical Engineering
Baltimore, MD 21218

8. PERFORMING ORGANIZATION REPORT NUMBER

9. SPONSORING/MONITORING AGENCY NAME(S) AND ADDRESS(ES)

Office of Naval Research
ONR 331
800 North Quincy Street
Arlington, VA 22217-5660

10. SPONSORING/MONITORING AGENCY REPORT NUMBER

11. SUPPLEMENTARY NOTES

12a. DISTRIBUTION/AVAILABILITY STATEMENT

Approved for public release:
Distribution unlimited.

12b. DISTRIBUTION CODE

13. ABSTRACT *(Maximum 200 words)*

The work summarized is divided into three parts. In Part I the development of a simplified model of thermo-acoustic devices is described and the results of its preliminary analysis documented. In Part II the results so far obtained in an experimental program designed for the visualization of flow and heat transfer in a thermoacoustic stack are described. Part III deals with the progress on a full Navier-Stokes numerical simulation of flow and heat transfer processes in the stack.

14. SUBJECT TERMS	15. NUMBER OF PAGES
Thermoacoustic, Refrigeration, Nonlinear Waves, Nonlinear Stability	36
	16. PRICE CODE

17. SECURITY CLASSIFICATION OF REPORT	18. SECURITY CLASSIFICATION OF THIS PAGE	19. SECURITY CLASSIFICATION OF ABSTRACT	20. LIMITATION OF ABSTRACT
UNCLASSIFIED	UNCLASSIFIED	UNCLASSIFIED	

DISCLAIMER NOTICE

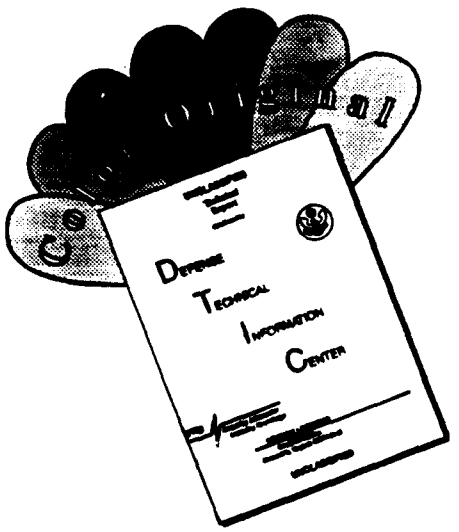

THIS DOCUMENT IS BEST QUALITY AVAILABLE. THE COPY FURNISHED TO DTIC CONTAINED A SIGNIFICANT NUMBER OF COLOR PAGES WHICH DO NOT REPRODUCE LEGIBLY ON BLACK AND WHITE MICROFICHE.

CONTENTS

Part I: Simplified model of thermoacoustic devices 1

I.1 Introduction 2
I.2 Simplified model of thermoacoustic devices 2
I.3 Energy relation and boundary conditions 3
I.4 Linear theory of simplified model 4
I.5 Weakly nonlinear theory 5
I.6 Numerical solution 10

Part II: Experimental effort 12

II.1 Introduction 13
II.2 Design of the experimental setup 13
II.3 Enlarged model of thermoacoustic devise 14
II.4 Instrumentation 19
II.5 Accomplishments 21
II.6 Future plans 22

Part III: Numerical modeling efforts 24

III.1 Objectives 25
III.1 Approach 25
III.1 Accomplishments 32

A. Prosperetti and M. Watanabe

SIMPLIFIED MODEL OF THERMO-ACOUSTIC DEVICES

1 Introduction

The analytical theory of thermoacoustic devices is well developed for the linear case. Theoretical work suitable to study higher amplitudes, however, is in its infancy (Gaitan and Atchley 1993).

To gain a better semi-quantative understanding of these processes as well as of other aspects of the design of thermoacoustics devices a simplified model suitable appears to be useful. The primary thrust of our work so far has been the development and study of such a model. A second aspect of our work has been the development of the exact linear thoery along alternative lines, again with an eye toward recasting the theory in a different form more suitable for extensions to the nonlinear case.

2 Simplified model of thermoacoustic devices

The key aspect of this model is to recast the governing equations in a form integrated over the cross-section of the thermoacoustic tube thus reducing the model to one dimension in space (along the tube axis) and time. Effects taking place along the orthogonal directions (friction, heat transfer, etc.) are to be accounted for by the introduction of suitable coefficients in the manner explained below.

Consider a linear thermoacoustic devices consisting of a duct of variable area $A(x)$. Upon integrating the equation of continuity over the volume delimited by two neighboring cross sections $A(x)$ and $A(x+dx)$ we find the well-known form

$$\frac{\partial < \rho >}{\partial t} + \frac{1}{A}\frac{\partial A < \rho u >}{\partial x} = 0\,, \tag{1}$$

where ρ is the gas density, u the velocity in the x-direction, and the angle brackets indicate the average over the cross section,

$$< \ldots > = \frac{1}{A(x)} \int_{A(x)} dA\,(\ldots)\,. \tag{2}$$

The condition of that the normal component of the exact velocity field vanishes on the lateral walls of the duct has been enforced in obtaining (1).

Similarly, the momentum equation in the x-direction becomes

$$\frac{\partial < \rho u >}{\partial t} + \frac{1}{A}\frac{\partial A < \rho u^2 >}{\partial x} + \frac{\partial < p >}{\partial x} + \frac{1}{A}(< p > - \overline{p})\frac{dA}{dx} = \frac{P}{A}(\overline{\tau \cdot \mathbf{n}})_x\,. \tag{3}$$

Here p is the gas pressure, τ the viscous stress tensor, and the overline denotes the average over the union $\mathcal{L}$ of the lines along which the cross-section A is cut by solid boundaries. In the unobstructed part of the duct this is just the perimeter of A but, when A is in the stack region for example, $\mathcal{L}$ would include all the "wetted" perimeter of the stack cross section. Thus, for example,

$$\overline{p} = \frac{1}{P}\oint_{\mathcal{L}} p\, d\ell \tag{4}$$

where P is the length of $\mathcal{L}$. The viscous component τ_{xx} has been neglected in deriving (3).

The last equation to consider is that for the gas enthalpy that, with the assumption of constant specific heat C_p, and the neglect of viscous heating, may be written in conservation form as

$$\frac{d}{dt}(\rho C_p T) - \frac{dp}{dt} + \rho C_p T\, \nabla \cdot \mathbf{u} = -\nabla \cdot \mathbf{q}\,, \tag{5}$$

where $d/dt \equiv \partial/\partial t + \mathbf{u} \cdot \nabla$ is the convective derivative and $\mathbf{q}$ is the heat flux vector. Before averaging this equation we note that, for a perfect gas,

$$\rho C_p T = \frac{\gamma}{\gamma - 1} p\,, \tag{6}$$

where γ is the adiabatic index, so that (5) becomes

$$\frac{dp}{dt} + \gamma p \nabla \cdot \mathbf{u} = -(\gamma - 1)\nabla \cdot \mathbf{q}. \tag{7}$$

Upon integration over the volume bounded by two neighboring cross sections we then have

$$\frac{\partial}{\partial t} < p > + \frac{1}{A} \langle \mathbf{u} \cdot \nabla p + \gamma p \nabla \cdot \mathbf{u} \rangle = -(\gamma - 1)\frac{P}{A}\overline{\mathbf{q} \cdot \mathbf{n}}. \tag{8}$$

To make progress we need to render the previous expressions more explicit. We start by noting that the pressure may be taken to be uniform over the cross section. This is true in view of the well-known properties of viscous boundary layers and also because in usual thermoacoustic devices the cross section of the system is small compared with the acoustic wavelength. With this approximation and writing p in place of $< p >$ we have

$$\langle \mathbf{u} \cdot \nabla p + \gamma p \nabla \cdot \mathbf{u} \rangle \simeq < u > \frac{\partial p}{\partial x} + \frac{\gamma p}{A} \nabla (A < u >), \tag{9}$$

and also $< p > - \overline{p} \simeq 0$. We further disregard correlation terms and write the average of products as products of averages,thus dropping the angle bracket notation. It should be noted that the error thus incurred is greater than that ensuing from the assuming p to be uniform. Although some correction could presumably be introduced to mitigate the error we do not do so as our objective here is to derive a simplified mathematical model. For the same reason we model the heat exchange between the gas and the surrounding structure (including the stack) in terms of a constant heat transfer coefficient per unit length H defined by

$$\frac{P}{A}\overline{\mathbf{q} \cdot \mathbf{n}} \equiv H(x)[T_w(x) - T], \tag{10}$$

where $T_w(x)$ is the temperature of the solid structure (e.g. the stack) at x. Ways to estimate H will be considered later. For the time being note that H can be a function of x to model different intensities of heat transfer, e.g. inside and outside the stack. In a similar spirit we introduce fluid-dynamic resistance coefficientper unit length by

$$\frac{P}{A}(\overline{\tau \cdot \mathbf{n}})_x \equiv -D(x)\, u. \tag{11}$$

With the preceding simplications and approximations the system of equations reduces to

$$\frac{\partial \rho}{\partial t} + \frac{1}{A}\frac{\partial A \rho u}{\partial x} = 0, \tag{12}$$

$$\rho\left(\frac{\partial u}{\partial t} + u\frac{\partial u}{\partial x}\right) + \frac{\partial p}{\partial x} = -D(x)\, u. \tag{13}$$

$$\frac{\partial p}{\partial t} + u\frac{\partial p}{\partial x} + \gamma \frac{p}{A}\frac{\partial (Au)}{\partial x} = (\gamma - 1)H[T_w(x) - T]. \tag{14}$$

To close this system, we further postulate that the averaged quantities satisfy the same equations of state as the corresponding exact ones, namely

$$p = R\rho T, \tag{15}$$

where R is the universal gas constant divided by the gas mass.

3 Energy relation and boundary conditions

The total energy of the system $\mathcal{E}$ is the sum of its internal and kinetic energies and, for a perfect gas, is given therefore by

$$\mathcal{E} = \int_{X(t)}^{L} dx\, A(x)\, \rho \left[C_v T + \frac{1}{2}u^2\right]. \tag{16}$$

Here it has been assumed that the left boundary oscillates around $x = 0$ with and instantaneous position $x = X(t)$. This would be the case if the device is operated as a refrigerator. For prime mover operation, on the other hand, $X = 0$.

Upon taking the time derivative and using the previous equations one readily finds

$$\frac{d\mathcal{E}}{dt} = \int_{X(t)}^{L} dx\, A(x)\left[H(T_w - T) - Du^2\right] + pA\dot{X}\Big|_{x=X(t)} . \tag{17}$$

For a rigid termination at $x = L$ the velocity must vanish. As a consequence of (13), this implies $\partial p'/\partial x = 0$ as well. If Eqs. (12) and (14) are then written at $x = L$, one finds

$$\left[\frac{\partial \rho}{\partial t} + \rho\frac{\partial u}{\partial x}\right]_{x=L} = 0\,, \tag{18}$$

$$\left[\frac{\partial p}{\partial t} + \gamma p\frac{\partial u}{\partial x} = (\gamma - 1)H[T_w(x) - T]\right]_{x=L} . \tag{19}$$

Upon eliminating $\partial u/\partial x$ one then finds, at $x = \mathrm{L}$,

$$\frac{\gamma}{\gamma - 1}\frac{p}{T}\frac{\partial T}{\partial t} = \frac{\partial p}{\partial t} + H(T_w - T)\,. \tag{20}$$

This relation shows that a knowledge of p at the boundary completely specifies T. No additional boundary conditions are therefore necessary.

The same argument applies at $x = 0$ in the prime mover case, which is the only one that we consider from now on.

4 Linear theory of simplified model

It is useful to consider the linear version of the previous model in the case of a duct of constant area with negligible dissipation. In this case Eqs. (12) become

$$\frac{\partial \rho'}{\partial t} + \frac{\partial \rho_0 u'}{\partial x} = 0\,, \tag{21}$$

$$\rho_0\frac{\partial u'}{\partial t} + \frac{\partial p'}{\partial x} = 0. \tag{22}$$

$$\frac{\partial p'}{\partial t} + \gamma p_0\frac{\partial u'}{\partial x} = -(\gamma - 1)HT'\,. \tag{23}$$

Here we have written

$$p = p_0 + p'\,, \qquad \rho = \rho_0 + \rho'\,, \qquad T = T_w + T'\,. \tag{24}$$

The subscripts 0 and the prime indicate unperturbed and perturbed quantities respectively. The unperturbed quantities satsify the equation of state with p_0 independent of x so that $\rho_0 = \rho_0(x)$ must compensate for the x-dependence of T_w.

It is easy to eliminate u' and T' from these equations to find

$$\frac{\partial}{\partial t}\left[\frac{\partial}{\partial x}\left(c_A^2\frac{\partial p'}{\partial x}\right) - \frac{\partial^2 p'}{\partial t^2}\right] + (\gamma - 1)\frac{H}{R\rho_0}\left[c_I^2\frac{\partial^2 p'}{\partial x^2} - \frac{\partial^2 p'}{\partial t^2}\right] = 0\,, \tag{25}$$

where c_A^2 and c_I^2 are the adiabatic and isothermal sound velocities given by

$$c_A^2 = \gamma R T_w\,, \qquad c_I^2 = RT_w\,. \tag{26}$$

Some insight into the behavior of the solutions o' the linear problem can be obtained by assuming oscillations with a (complex) frequency ω, $p' = P(x)\exp i\omega t$. With this assumption the previous equation becomes

$$i\omega\left[\frac{\partial}{\partial x}\left(c_A^2\frac{\partial P}{\partial x}\right)+\omega^2 P\right]+(\gamma-1)\frac{H}{R\rho_0}\left[c_I^2\frac{\partial^2 P}{\partial x^2}+\omega^2 P\right]=0\,. \tag{27}$$

Upon multiplication by $\overline{P}$ (where the overline denotes the complex conjugate), integration from 0 to L, and use of the fact that $\partial P/\partial x$ vanishes at $x = 0$, L, we find an expression of the form

$$i\omega(A\omega^2 - C) + B\omega^2 - D = 0\,, \tag{28}$$

where

$$A = \int_0^L |P|^2 dx \qquad B = \frac{\gamma-1}{p_0}\int_0^L HT_w|P|^2 dx\,, \tag{29}$$

$$C = \int_0^L c_A^2\left|\frac{\partial P}{\partial x}\right|^2 dx\,, \qquad D = -\frac{(\gamma-1)R}{p_0}\int_0^L HT_w^2\overline{P}\frac{\partial^2 P}{\partial x^2}\,. \tag{30}$$

It may be noted that D is in general a complex quantity with real and imaginary parts given by

$$D_r \equiv Re\{D\} = \frac{(\gamma-1)R}{2p_0}\int_0^L\left[\frac{d}{dx}(HT_w^2)\frac{d|P|^2}{dx}+2HT_w^2\left|\frac{dP}{dx}\right|^2\right]dx\,, \tag{31}$$

$$D_i \equiv Im\{D\} = \frac{(\gamma-1)R}{2ip_0}\int_0^L\frac{d}{dx}(HT_w^2)\left(\overline{P}\frac{dP}{dx}-P\frac{d\overline{P}}{dx}\right)dx\,. \tag{32}$$

Equation (28) in general has three complex roots, so that p' is the superposition of three different modes. For any of these modes to have the nature of steady oscillations it is necessary that ω be purely real. In this case, upon separating real and imaginary parts, we have from (28)

$$\omega(A\omega^2 - C) - D_i = 0\,, \qquad B\omega^2 - D_r = 0\,. \tag{33}$$

It is clear from the second of these equations that only two such roots can exist, one the opposite of the other. For the first relation to be satisfied, it is then necessary that $D_i = 0$. Furthermore, since B is patently positive definite, for the hypothesized real roots to exist, it is also necessary that $D_r \geq 0$. It is seen from (31) that D_r is the sum of a positive definite term and a term that can be positive or negative. The requirement $D_r \geq 0$ therefore implies that the latter term

$$J \equiv \int_0^L \frac{d}{dx}(HT_w^2)\frac{d|P|^2}{dx}dx\,, \tag{34}$$

not be too negative.

When the two equations (33) are compatible, it is readily shown that it follows from (28) that the third root is purely imaginary and is given by

$$i\omega = -\frac{B}{A}\,. \tag{35}$$

Since, as is clear from their definition, both A and B are positive definite, the mode corresponding to this root is always exponentially damped.

5 Weakly nonlinear theory

We now present some preliminary results of a weakly nonlinear analysis of the simplified model for the constant-area case.

In the first place, it is useful to eliminate the density by using the equation of state to find

$$T\frac{\partial p}{\partial t} - p\frac{\partial T}{\partial t} + pT\frac{\partial u}{\partial x} + uT\frac{\partial p}{\partial x} - up\frac{\partial T}{\partial x} = 0$$
$$p\frac{\partial u}{\partial t} + pu\frac{\partial u}{\partial x} + RT\frac{\partial p}{\partial x} = 0$$
$$\frac{\partial p}{\partial t} + u\frac{\partial p}{\partial x} + \gamma p\frac{\partial u}{\partial x} = (\gamma - 1)H\,(T_w - T)$$

Furthermore, by combining the second and third equations of this set according to

$$RT_w\frac{\partial}{\partial x}(\text{Energy}) - \frac{\partial}{\partial t}(\text{Momentum})$$

we find the wave equation

$$\begin{aligned}
&\gamma RT_w p\frac{\partial^2 u}{\partial x^2} - p\frac{\partial^2 u}{\partial t^2} \\
&= \frac{\partial p}{\partial t}\left(\frac{\partial u}{\partial t} + u\frac{\partial u}{\partial x}\right) + p\frac{\partial u}{\partial t}\frac{\partial u}{\partial x} + pu\frac{\partial^2 u}{\partial x\partial t} + R\frac{\partial T}{\partial t}\frac{\partial p}{\partial x} + R\,(T - T_w)\,\frac{\partial^2 p}{\partial x\partial t} \\
&\quad -RT_w\frac{\partial u}{\partial x}\frac{\partial p}{\partial x} - RT_w u\frac{\partial^2 p}{\partial x^2} - \gamma RT_w\frac{\partial p}{\partial x}\frac{\partial u}{\partial x} + (\gamma - 1)H\,RT_w\frac{\partial}{\partial x}\,(T_w - T)\,.
\end{aligned}$$

We now proceed in the usual way introducing the slow times

$$\tau = \epsilon t\,, \qquad \theta = \epsilon^2 t\,, \tag{36}$$

where ϵ is a measure of the amplitude of the wave, and expanding all the fields in powers of ϵ, e.g $u = \epsilon u_1 + \epsilon^2 u_2 + \epsilon^3 u_3 + \ldots$. Furthermore, we also let

$$(\gamma - 1)\,H \;=\; h_0 + \epsilon h_1 + \epsilon^2 h_2 + \ldots\,. \tag{37}$$

Upon separating the various orders in ϵ we have:

Order ϵ

$$\begin{aligned}
T_w\frac{\partial p_1}{\partial t} - p_0\frac{\partial T_1}{\partial t} + p_0 T_w\frac{\partial u_1}{\partial x} - p_0\frac{dT_w}{dx}u_1 &= 0 \\
p_0\frac{\partial u_1}{\partial t} + RT_w\frac{\partial p_1}{\partial x} &= 0 \\
\frac{\partial p_1}{\partial t} + \gamma p_0\frac{\partial u_1}{\partial x} &= 0 \\
\gamma RT_w p_0\frac{\partial^2 u_1}{\partial x^2} - p_0\frac{\partial^2 u_1}{\partial t^2} &= -RT_w h_0\frac{\partial T_1}{\partial x}
\end{aligned}$$

Order ϵ^2

$$\begin{aligned}
&T_w\frac{\partial p_2}{\partial t} - p_0\frac{\partial T_2}{\partial t} + p_0 T_w\frac{\partial u_2}{\partial x} - p_0\frac{dT_w}{dx}u_2 \\
&= \left[-T_w\frac{\partial p_1}{\partial \tau} + p_0\frac{\partial T_1}{\partial \tau}\right] - T_1\frac{\partial p_1}{\partial t} + p_1\frac{\partial T_1}{\partial t} - (p_0 T_1 + p_1 T_w)\frac{\partial u_1}{\partial x} - T_w\frac{\partial p_1}{\partial x}u_1 + \left(p_0\frac{\partial T_1}{\partial x} + p_1\frac{dT_w}{dx}\right)u_1 \\
&p_0\frac{\partial u_2}{\partial t} + RT_w\frac{\partial p_2}{\partial x}
\end{aligned}$$

$$= \left[-p_0\frac{\partial u_1}{\partial \tau}\right] - p_1\frac{\partial u_1}{\partial t} - p_0u_1\frac{\partial u_1}{\partial x} - RT_1\frac{\partial p_1}{\partial x}$$

$$\frac{\partial p_2}{\partial t} + \gamma p_0\frac{\partial u_2}{\partial x}$$

$$= \left[-(h_0T_2 + h_1T_1) - \frac{\partial p_1}{\partial \tau}\right] - u_1\frac{\partial p_1}{\partial x} - \gamma p_1\frac{\partial u_1}{\partial x}$$

$$\gamma RT_w p_0\frac{\partial^2 u_2}{\partial x^2} - p_0\frac{\partial^2 u_2}{\partial t^2}$$

$$= \left[2p_0\frac{\partial^2 u_1}{\partial \tau \partial t}\right] - \gamma R\frac{\partial^2 u_1}{\partial x^2}(T_1p_0 + T_wp_1) + p_1\frac{\partial^2 u_1}{\partial t^2}$$
$$+\frac{\partial p_1}{\partial t}\frac{\partial u_1}{\partial t} + p_0\frac{\partial u_1}{\partial t}\frac{\partial u_1}{\partial x} + p_0u_1\frac{\partial^2 u_1}{\partial x \partial t} + R\frac{\partial T_1}{\partial t}\frac{\partial p_1}{\partial x} + RT_1\frac{\partial^2 p_1}{\partial t \partial x}$$
$$-RT_w\frac{\partial u_1}{\partial x}\frac{\partial p_1}{\partial x} - RT_wu_1\frac{\partial^2 p_1}{\partial x^2} - \gamma RT_w\frac{\partial p_1}{\partial x}\frac{\partial u_1}{\partial x} - RT_w\left[h_0\frac{\partial T_2}{\partial x} + h_1\frac{\partial T_1}{\partial x}\right]$$

Order ϵ^3

$$p_0\frac{\partial u_3}{\partial t} + RT_w\frac{\partial p_3}{\partial x}$$

$$= -p_0\left[\frac{\partial u_1}{\partial \theta} + \frac{\partial u_2}{\partial \tau}\right] - \left(p_1\frac{\partial u_2}{\partial t} + p_2\frac{\partial u_1}{\partial t}\right) - p_0\left(u_1\frac{\partial u_2}{\partial x} + u_2\frac{\partial u_1}{\partial x}\right) - R\left(T_1\frac{\partial p_2}{\partial x} + T_2\frac{\partial p_1}{\partial x}\right) - p_1u_1\frac{\partial u_1}{\partial x}$$

$$\frac{\partial p_3}{\partial t} + \gamma p_0\frac{\partial u_3}{\partial x}$$

$$= \left[-(h_0T_3 + h_1T_2 + h_2T_1) - \left(\frac{\partial p_1}{\partial \theta} + \frac{\partial p_2}{\partial \tau}\right)\right] - \left(u_1\frac{\partial p_2}{\partial x} + u_2\frac{\partial p_1}{\partial x}\right) - \gamma\left(p_1\frac{\partial u_2}{\partial x} + p_2\frac{\partial u_1}{\partial x}\right)$$

$$\gamma RT_w p_0\frac{\partial^2 u_3}{\partial x^2} - p_0\frac{\partial^2 u_3}{\partial t^2}$$

$$= \left[2p_0\frac{\partial^2 u_1}{\partial \theta \partial t} + p_0\frac{\partial^2 u_1}{\partial \tau^2} + 2p_0\frac{\partial^2 u_2}{\partial \tau \partial t} + p_1\frac{\partial^2 u_1}{\partial \tau \partial t}\right] + p_1\frac{\partial^2 u_2}{\partial t^2} + p_2\frac{\partial^2 u_1}{\partial t^2}$$
$$+\left[\frac{\partial p_1}{\partial t}\frac{\partial u_1}{\partial \tau} + \frac{\partial p_1}{\partial \tau}\frac{\partial u_1}{\partial t} + p_0\frac{\partial u_1}{\partial x}\frac{\partial u_1}{\partial \tau} + p_0u_1\frac{\partial^2 u_1}{\partial x \partial \tau} + R\frac{\partial p_1}{\partial x}\frac{\partial T_1}{\partial \tau} + RT_1\frac{\partial^2 p_1}{\partial \tau \partial x}\right] - \gamma RT_w\left(p_1\frac{\partial^2 u_2}{\partial x^2} + p_2\frac{\partial^2 u_1}{\partial x^2}\right)$$
$$+\frac{\partial p_1}{\partial t}\left(\frac{\partial u_2}{\partial t} + u_1\frac{\partial u_1}{\partial x}\right) + \frac{\partial p_2}{\partial t}\frac{\partial u_1}{\partial t} + p_0\frac{\partial u_1}{\partial x}\frac{\partial u_2}{\partial t} + p_0\frac{\partial u_2}{\partial x}\frac{\partial u_1}{\partial t} + p_1\frac{\partial u_1}{\partial x}\frac{\partial u_1}{\partial t}$$
$$+p_0u_1\frac{\partial^2 u_2}{\partial x \partial t} + p_0u_2\frac{\partial^2 u_1}{\partial x \partial t} + p_1u_1\frac{\partial^2 u_1}{\partial x \partial t} + R\frac{\partial p_1}{\partial x}\frac{\partial T_2}{\partial t} + R\frac{\partial p_2}{\partial x}\frac{\partial T_1}{\partial t}$$
$$+R\left(T_1\frac{\partial^2 p_2}{\partial t \partial x} + T_2\frac{\partial^2 p_1}{\partial t \partial x}\right) - RT_w\left(\frac{\partial u_2}{\partial x}\frac{\partial p_1}{\partial x} + \frac{\partial u_1}{\partial x}\frac{\partial p_2}{\partial x}\right) - RT_w\left(u_1\frac{\partial^2 p_2}{\partial x^2} + u_2\frac{\partial^2 p_1}{\partial x^2}\right)$$
$$-\gamma RT_w\left(\frac{\partial p_1}{\partial x}\frac{\partial u_2}{\partial x} + \frac{\partial p_2}{\partial x}\frac{\partial u_1}{\partial x}\right) - RT_w\left[h_0\frac{\partial T_3}{\partial x} + h_1\frac{\partial T_2}{\partial x} + h_2\frac{\partial T_1}{\partial x}\right]$$

The analysis of this system is rather complex and is still under way. To demonstrate the procedure, we consider here the simplest case of very weak heat transfer.

Very weak heat transfer

To study this case we set $h_0 = 0$, $h_1 = 0$. We start by considering the Sturm-Liouville problem

$$\frac{d^2v_n}{dx^2} + \lambda_n\sigma(x)v_n(x) = 0$$

$$v(0) = v(L) = 0\,, \tag{38}$$

where the index n labels the different eigenvalues and eigenfunctions and

$$\sigma = \frac{1}{\gamma R T_w}\,.$$

Upon considering the problems for n and m and combining we have

$$v_m\left[v_n'' + \lambda_n \sigma v_n\right] - v_n\left[v_m'' + \lambda_m \sigma v_m\right] = 0$$

$$\left(\lambda_n - \lambda_m\right)\sigma v_n v_m + v_m v_n'' - v_n v_m'' = 0$$

Integrate over the range the last two terms to find

$$\begin{aligned}\int_0^L \left(v_m v_n'' - v_n v_m''\right) dx &= \left[v_m v_n' - v_n v_m'\right]_0^L - \int_0^L \left(v_n' v_m' - v_m' v_n'\right) dx \\ &= \left[v_m v_n' - v_n v_m'\right]_0^L \\ &= 0\end{aligned}$$

The boundary conditions (38) were used in the last step. Then we have

$$\left(\lambda_n - \lambda_m\right)\int_0^L \sigma v_n v_m dx = 0$$

which proves orthogonality of the eigenfunctions corresponding to distinct eigenvalues,

$$\left(v_n, v_m\right) \equiv \int_0^L \sigma v_n v_m dx = 0 \text{ if } \lambda_n \neq \lambda_m \tag{39}$$

Let us now turn to the wave equation (38) to $O(\epsilon)$, which is in the present case

$$\gamma R T_w \frac{\partial^2 u_1}{\partial x^2} - \frac{\partial^2 u_1}{\partial t^2} = 0 \tag{40}$$

We write the solution in the form

$$u_1 = A_1(\tau, \theta) v_1(x) \exp(\omega t) + c.c.\,, \tag{41}$$

where $c.c.$ denotes the complex conjugate, $v_1(x)$ is the first eigenvector of the Sturm-Liouville problem, and $\lambda_1 = \omega^2$ the first eigenvalue. Note that v_1 can be taken real and normalized to 1 according to the scalar product (39). From the linearized equations we then have

$$\begin{aligned}\frac{\partial^2 u_1}{\partial x^2} &= -\frac{\omega^2}{\gamma R T_w} u_1 \\ p_1 &= \frac{\imath}{\omega}\gamma p_0 \frac{\partial u_1}{\partial x} + c.c. \\ \frac{\partial p_1}{\partial x} &= -\imath\omega \frac{p_0}{R T_w} u_1 + c.c. \\ \frac{\partial^2 p_1}{\partial x^2} &= -\imath\omega \frac{p_0}{R T_w}\left(\frac{\partial u_1}{\partial x} - \frac{T_w'}{T_w} u_1\right) + c.c. \\ T_1 &= \frac{\imath}{\omega}\left[(\gamma - 1) T_w \frac{\partial u_1}{\partial x} + T_w' u_1\right] + c.c.\end{aligned}$$

where $T_w' \equiv dT_w/dx$.

Upon substitution of the previous expressions for the first-order fields, the wave equation (38) for u_2 becomes

$$\gamma RT_w \frac{\partial^2 u_2}{\partial x^2} - \frac{\partial^2 u_2}{\partial t^2} = \left[2p_0 \frac{\partial^2 u_1}{\partial \tau \partial t}\right] + \omega p_0 \left(2(\gamma-1)v_1 v_1' + \frac{T_w'}{T_w} v_1 v_1\right)\left[A_1^2 \exp(2\imath\omega t) - c.c.\right]$$

The terms in the second line drive oscillations at frequency 2ω, which is not an eigenfrequency of the operator in the left-hand side. Hence, in order to avoid secular terms, it is necessary and sufficient to impose that the term in brackets vanish,

$$\frac{\partial u_1}{\partial \tau} = 0$$

so that $A_1(\tau, \theta) = A_1(\theta)$. The method of variation of constants enables us now to determine the solution for u_2 which can be shown to have the form

$$u_2 = \imath A_1(\theta)^2 v_2(x) \exp(\imath\omega t) + c.c. \tag{42}$$

where $v_2(x)$ is a real function.

At the next order we are only interested in the terms in the right-hand side of the wave equation (38) that may induce a resonant response, i.e. the terms proportional to $\exp \pm\imath\omega t$. Upon writing explicitly only such terms, the third-order wave equaition becomes

$$\begin{aligned}
&\gamma RT_w \frac{\partial^2 u_3}{\partial x^2} - \frac{\partial^2 u_3}{\partial t^2} \\
&= 2\imath\omega p_0 \frac{\partial u_1}{\partial \theta} - RT_w h_2 \frac{\partial T_1}{\partial x} \\
&\quad -\imath\omega p_0 \left[(4-3\gamma)\frac{\partial \tilde{u}_1}{\partial x} u_2 - \frac{9T_w'}{2T_w}\tilde{u}_1 u_2 + 2\tilde{u}_1 \frac{\partial u_2}{\partial x}\right] \\
&\quad -p_0 \tilde{u}_1 \left[\frac{\gamma(\gamma+5)}{2}\left(\frac{\partial u_1}{\partial x}\right)^2 + \frac{u_1^2}{T_w}\left(\frac{\omega^2}{2\gamma R}(\gamma+1) + \frac{T_w''}{2} - \frac{3T_w'^2}{T_w}\right) + \frac{\partial u_1}{\partial x} u_1 \frac{4-\gamma}{2}\frac{T_w'}{T_w}\right] + c.c. \\
&= 2\imath\omega p_0 v_1 \frac{\partial A_1}{\partial \theta} - \frac{\imath}{\omega} h_2 \left[\gamma RT_w T_w' v_1' + RT_w T_w'' v_1 - \frac{\gamma-1}{\gamma}\omega^2 T_w v_1\right] \\
&\quad +\omega p_0 A_1^2 \tilde{A}_1 \left\{(4-3\gamma)v_1' v_2 - \frac{9T_w'}{2T_w} v_1 v_2 + 2v_1 v_2'\right\} \\
&\quad -p_0 A_1^2 \tilde{A}_1 v_1 \left[\frac{\gamma(\gamma+5)}{2} v_1'^2 + \frac{v_1^2}{T_w}\left\{\frac{\omega^2}{2\gamma R}(\gamma+1) + \frac{T_w''}{2} - \frac{3T_w'^2}{T_w}\right\} + v_1 v_1' \frac{4-\gamma}{2}\frac{T_w'}{T_w}\right] + c.c.
\end{aligned}$$

In order to avoid secular terms, the right-hand side must be orthogonal to v_1 in the sense of the scalar product (39). This condition readily leads to

$$\frac{\partial A_1}{\partial \theta} = \frac{h_2}{2\omega^2 p_0} Q_r A_1 - \frac{\imath}{2\omega} Q_i A_1^2 \tilde{A}_1 \tag{43}$$

and to the complex conjugate of this equation. Here

$$\begin{aligned}
Q_r &= \left(v_1, \gamma RT_w T_w' v_1' + RT_w T_w'' v_1 - \frac{\gamma-1}{\gamma}\omega^2 T_w v_1\right) \\
Q_i &= \omega\left(v_1, (4-3\gamma)v_1' v_2 - \frac{9T_w'}{2T_w} v_1 v_2 + 2v_1 v_2'\right) \\
&\quad - \left(v_1, \frac{\gamma(\gamma+5)}{2} v_1'^2 v_1 + \left[\frac{\omega^2}{2\gamma R}(\gamma+1) + \frac{T_w''}{2} - \frac{3T_w'^2}{T_w}\right]\frac{v_1^3}{T_w} + \frac{4-\gamma}{2}\frac{T_w'}{T_w} v_1' v_1^2\right).
\end{aligned}$$

Clearly, the second term of (43) describes a slight shift of the linear frequency. The first term instead indicates the possibility for damping ($Q_r < 0$), or amplification ($Q_r > 0$) of the linear steady oscillations.

6 Numerical solution

The weakly nonlinear analysis previously described is very cumbersome and we found it useful to calculate some numerical solutions in parallel with it. For this purpose we have taken H = constant and we have assumed a hyperbolic-tangent distribution of the wall temperature,

$$T_w = T_L + \left[1 + \tanh\, 1.83178 \frac{2x/L - 0.5}{0.2}\right] \frac{1}{2}(T_H - T_L)\,. \tag{44}$$

Here the coordinate system used is such that the tube extends between $-\frac{1}{2}L$ and $\frac{1}{2}L$, with $L = 1$ m. Figure 1 shows the pressure (in atmospheres) at the left-end of the tube as a function of the dimensionless time

$$t_* = \frac{1}{2L}\sqrt{\frac{1}{2}\gamma R(T_H + T_L)} \tag{45}$$

for $L = 1$ m, $H = 10$ W/m K, $T_L = 250$ K, $T_H = 1400$ K. After an initial transient, the result very nearly stabilizes around a finite amplitude. An example of the pressure distribution in these steady state conditions is shown in Fig. 2.

If the higher temperature is increased to $T_H = 1900$ K, for the same values of H, L, and T_L, the resulting pressure-versus-time is as shown in Fig. 3, and the pressure profile in the tube at a particular instant as shown in Fig. 4. The oscillations exhibited in this case are clearly a numerical artifact due to the use of upwind differencing in the spatial discretization of the equations. This problem is well known to occur in the neighborhood of shock fronts. A new class of numerical methods, called total-variation-diminishing, has been developed to avoid it. We are currently implementing one such technique to be able to extend the calculation to higher-amplitude oscillations.

Reference

GAITAN, D.F. AND ATCHLEY, A.A. 1993 Finite amplitude standing waves in harmonic and anharmonic tubes. *J. Acoust. Soc. Am.* **93** 2489-2495.

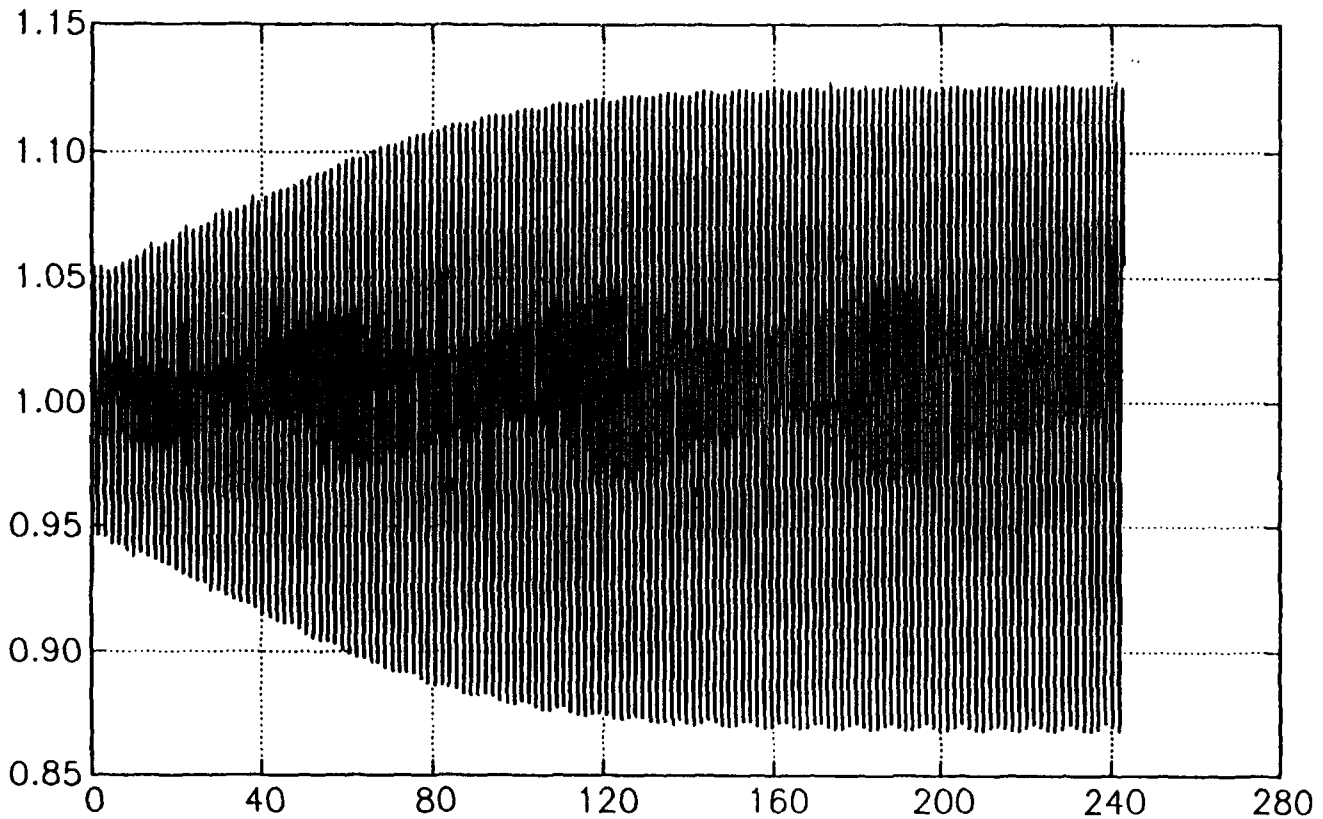

Fig. 1. Pressure at the left wall of the tube (in atmospheres) versus the nondimensional time defined by (45) for the temperature distribution given by Eq. (44) with $T_L = 250$ K, $T_H = 1400$ K, $H = 10$ W/mK, $L = 1$ m.

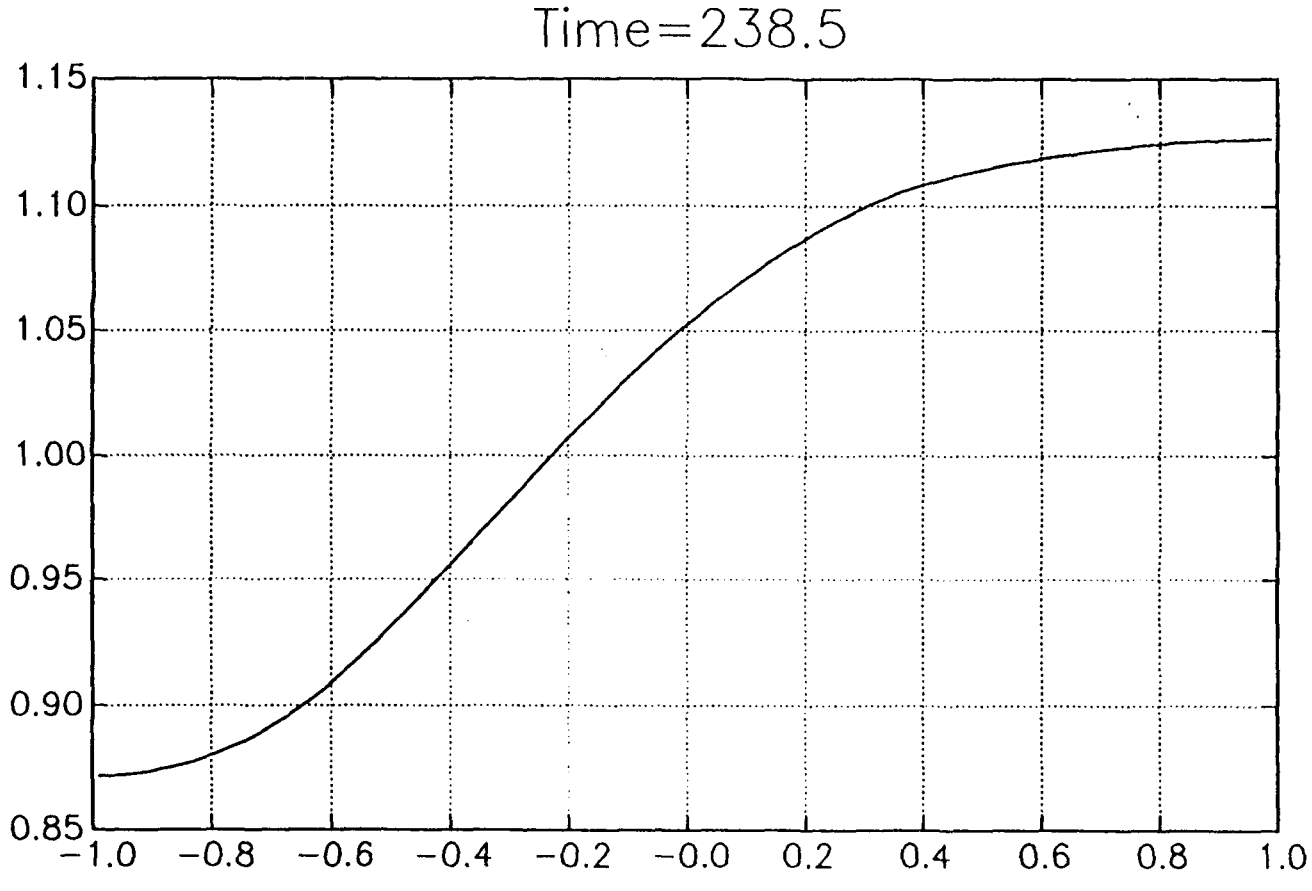

Fig. 2. Pressure distribution (in atmospheres) for the case of the previous figure at the dimensionless time $t_* = 238.5$.

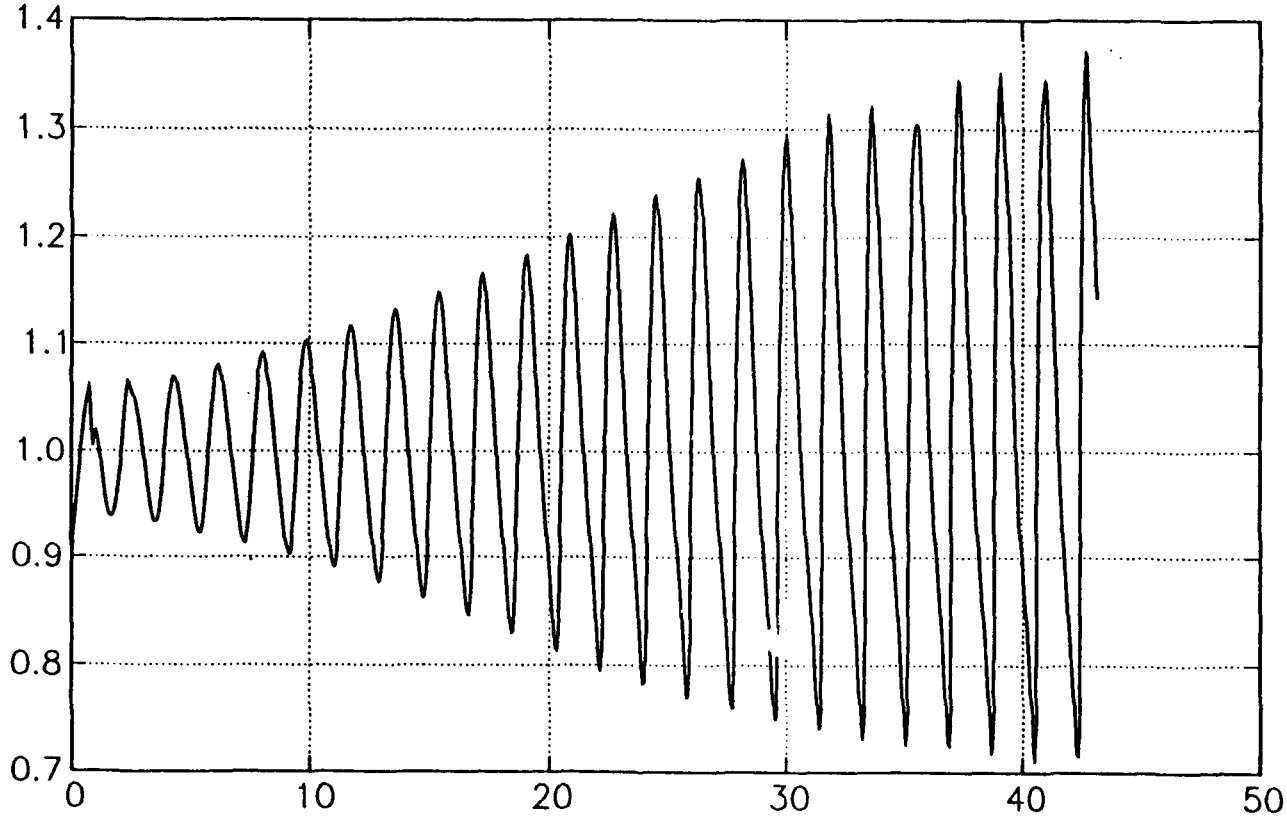

Fig. 3. Same as Fig. 1 for a hot-end temperature $T_H = 1900$ K.

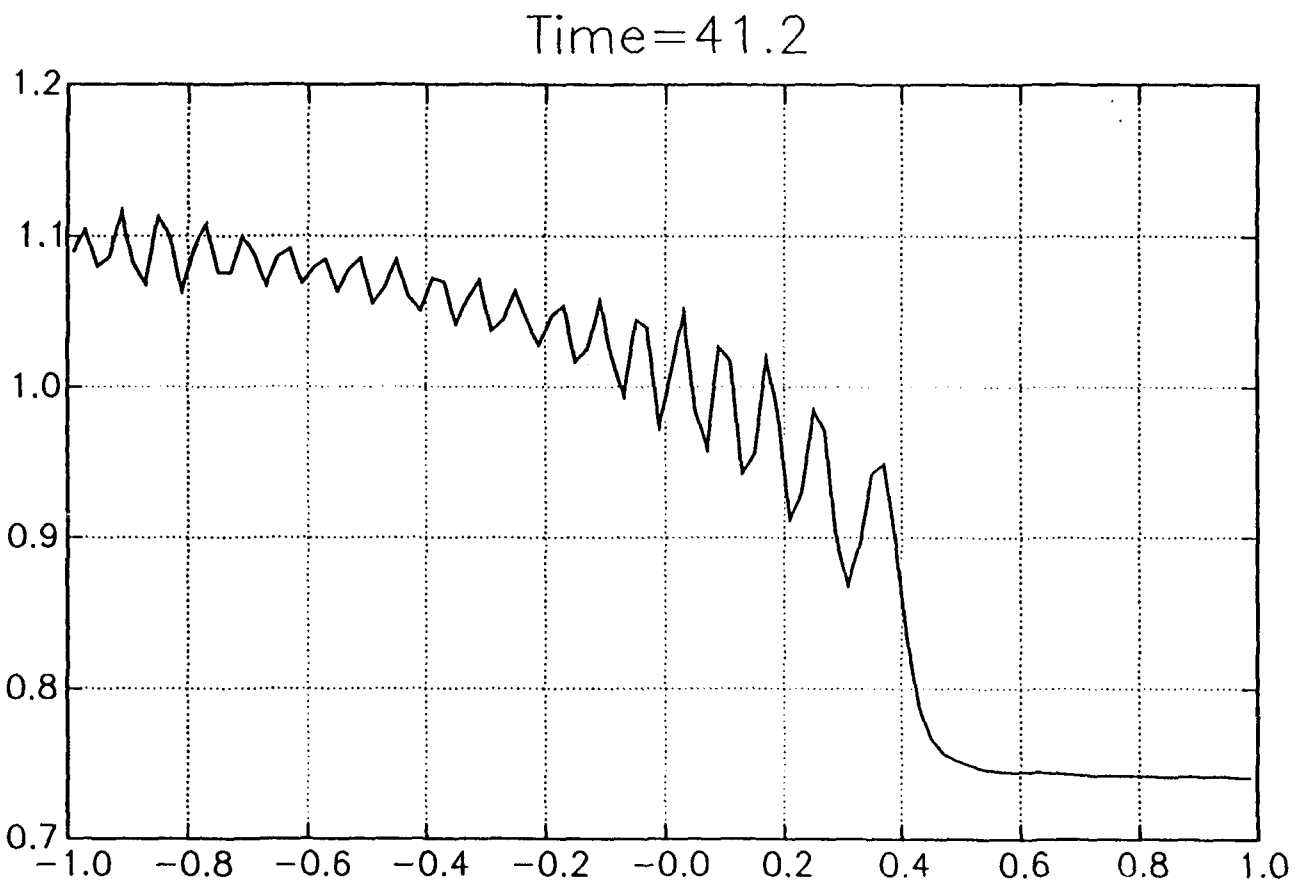

Fig. 4. Pressure distribution (in atmospheres) for the case of Fig. 3 at the dimensionless time $t_* = 41.2$. The oscillations are unphysical and due to the development of a shock wave. This problem will be corrected by means of a Total Variation Diminishing numerical scheme.

C. Herman and C. Bartscher

EXPERIMENTAL EFFORT

1. INTRODUCTION

The main objective of the experimental work is to uncover the factors limiting the performance of existing designs of thermoacoustic devices by gaining better insight into the flow structure and the heat transfer mechanisms. This will be achieved by using different visualization techniques, such as smoke injection, holographic interferometry and thermochromatic liquid crystals. Visualization techniques will provide the necessary information on the local flow and temperature fields in the regions of interest in addition to the conventional measurements of temperatures, pressures and other operating parameters in different parts of the thermoacoustic device. The measurements to be performed during the present study differ from those described in literature, and the requirements imposed by the different visualization measurements require specific design solutions for the experimental setup. The specific design requirements and procedures are described in this report.

2. DESIGN OF THE EXPERIMENTAL SETUP

The **design tasks** for the setups to be used in the experimental investigation of thermoacoustic phenomena are twofold:

1. In the first step of the experimental investigations, an **enlarged model** of a thermoacoustic device, suitable for visualization of the oscillatory temperature fields by holographic interferometry, was built. The model was designed so that, with minor modifications, it can function both as a heat pump and a prime mover. The design also allows the visualization of the flow fields by smoke injection and the visualization of the temperature distribution on the stack plates using thermochromatic liquid crystals.
2. At a more advanced stage of the research (second year), after satisfactory results have been obtained in the experiments with the enlarged model, a **real thermoacoustic device** suitable for accurate measurements will be built. The design should be modular in order to allow the modification and exchange of its key parts. In this way, it will be possible to investigate modifications proposed during the course of the research on the actual device. Again, an attempt will be made to build a device which can function both as a prime mover and a heat pump. This device will be suitable for the investigation of the phenomenon of thermoacoustic streaming.

In addition to the two experimental setups, a **thermoacoustic couple**, suitable for temperature measurements both in the thermoacoustic device and in the model, will be designed. Measurements and visualization experiments with the thermoacoustic couple only will be performed to analyze heat transfer and fluid flow phenomena on a short stack. The thermoacoustic couple will be designed to allow visualization experiments with smoke injection as well as interferometric measurements.

3. ENLARGED MODEL OF A THERMOACOUSTIC DEVICE

3.1 Design requirements

Both standard requirements related to the operation of thermoacoustic devices and specific ones, which allow visualization measurements, have to be met in the design of the experimental setup. The most important criteria for the design of the enlarged thermoacoustic device model are as follows.

1. A **modular structure** allows the experimenter to disassemble the device completely and easily in order to exchange its key parts. In this way, the flexibility to investigate a variety of heat transfer and fluid flow phenomena under different operating conditions is achieved. At this stage, we must keep in mind that the need to investigate new effects may arise in different phases of the research.
2. In order to allow measurements by holographic interferometry, the flow and temperature fields in the investigated region should be two-dimensional. This is achieved by designing the experimental setup in such a way, that the **cross section** of the resonance tube is **rectangular**. However, all thermoacoustic devices previously described in literature have a circular cross section. The temperature in the tube is constant along the paths of the laser light used for transillumination of the measurement volume. The requirements for holographic interferometry define the spanwise dimension of the tube. For the temperature differences expected in the experiments, a spanwise dimension of 15 cm is required. The height of the tube is determined by the maximum efficient diameter of the expanded laser beam, which is about 5 cm. Using the above criteria, the dimensions of the cross section of the resonance tube are selected to be
   - height of tube: h 0.05 m
   - width of tube: w 0.15 m
3. The **plates of the stack are parallel** in order to achieve approximately two-dimensional temperature fields in the region of interest. The minimum spacing between the stack plates is determined by the resolution of holographic interferometry. In our investigations, this spacing is determined to be 5 mm.
4. The **viewing windows** allow the visualization of a region of 8 cm in diameter, which corresponds to the diameter of the expanded laser beam. The region of interest for visualization of flow and temperature fields includes the stack and the channel region in the vicinity of the stack, and is approximately 12 cm long. As the dimension of this region is larger than the diameter of the expanded laser beam, one half of this region is investigated at a time. Two sets of interferometric images and the corresponding viewing windows are necessary in order to record temperature fields along the whole stack and in its vicinity. The direction of transillumination is indicated in the schematic of the experimental setup in Figure 1.
5. The **tube walls** in the region of the stack and the **stack plates are transparent** to allow flow visualization by smoke injection as well as the measurement of temperatures of the stack plates by coating them with thermochromatic liquid crystals. In both of these measurements, the direction of transillumination is perpendicular to that during interferometric measurements, as indicated in Figure 1.

6. The channel will be built with a **closed end.** and with constant cross section of the resonance tube. The selected design allows the variation of the tube length, if necessary.
7. The model operates with **air at atmospheric pressure** as the working fluid. For the design calculations, the following thermophysical properties of air are assumed
   - mean temperature: T_m 293 K
   - ratio of specific heat: γ 1. 40
   - specific gas constant: R 286.6 J/Kg K
   - velocity of sound: c_{air} 342.9 m/s
8. Apart from the visualization measurements, pressure measurements (to obtain information on losses in the acoustic field due to the stack and the heat exchangers), temperature measurements - with thermocouples - along the surface of the tube (to account for heat losses), temperature measurements in the heat exchangers and near the acoustic driver, and **other measurements** are necessary.

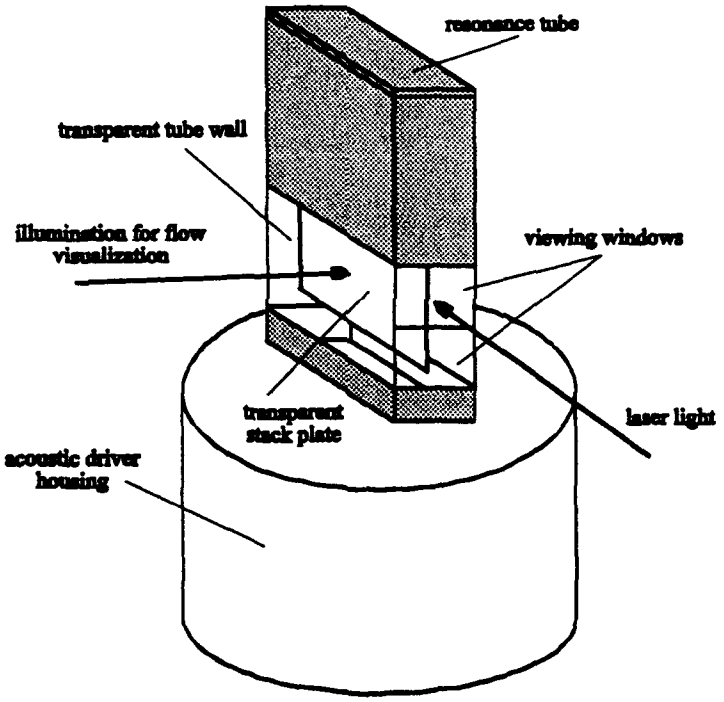

Figure 1. Schematic of the thermoacoustic device model with viewing directions for visualization measurements

3.2 Acoustic driver

A commercial loudspeaker, an 8" woofer, is used as acoustic driver (Peerless - type 832556). The most important technical data for the selected loudspeaker are the following:

- frequency range: f 20 - 5000 Hz
- resonant frequency: F_0 30.9/32.3 Hz
- effective cone diameter: d 0.153 m
- max. linear SPL: 108 dB/85 W

3.3 Calculation of the length of the resonance tube and the frequency range

With the assumptions discussed in the previous sections, it is possible to perform the necessary calculations to determine the limiting dimensions of the resonance tube and to verify that the selected loudspeaker can deliver the required acoustic power input.

Minimum and maximum tube length

a) Plane acoustic wave condition. For better efficiency, plane acoustic wave fronts are preferred during the operation of the thermoacoustic device. In order to achieve this, the diameter of the tube must be sufficiently small compared to the dimensions of the loudspeaker, and the ratio of the wavelength of the sound wave to the diameter of the tube must be greater than six [1]. As the cross section of the resonance tube is rectangular, the larger dimension (width of the tube, w=0.15 m) is selected as representative value for the diameter. For this situation, the minimum wavelength is determined to be

$$\frac{\lambda}{w} \geq 6 \Rightarrow \lambda_{min} = 0.90 \text{ m}.$$

b) Maximum frequency for a flat reproduction. The loudspeaker has perfect compensation, and achieves a "flat" response up to a specific maximum frequency. The following equation shows, that an increase of the loudspeaker diameter d results in a decrease of the available maximum frequency for the flat reproduction [2].

$$f_{max} = \frac{c_{air}}{4\pi\frac{1}{2}d} = \frac{342.9\frac{m}{s}}{4\pi\frac{1}{2}0.153m} = 356.69 \text{ Hz}$$

Thus, the upper frequency limit in order to achieve a flat reproduction is 356 Hz for the selected loudspeaker with a diameter d=0.153 m. This calculation holds for a temperature of 293 K only. As the velocity of sound is dependent on the temperature, the value for the frequency will also change.

c) Minimum tube length. From the maximum frequency, the lower limit for the tube length l is determined at room temperature from the following equations:

$$\lambda_{min} = \frac{c_{air}}{f_{max}} = \frac{342.9\frac{m}{s}}{356.69Hz} = 0.96 \text{ m} \quad \text{and} \quad l_{tube,min} = \frac{1}{2}\lambda_{min} = 0.48 \text{ m}$$

d) Maximum tube length. As the resonant frequency for speaker-type 832556 is 32.9 Hz, the minimum frequency f_{min} = 35 Hz is used in the calculation.

$$\lambda_{max} = \frac{c_{air}}{f_{min}} = \frac{343.11\frac{m}{s}}{35\frac{1}{s}} = 9.80 \text{ m} \quad \text{and} \quad l_{tube,max} = \frac{1}{2}\lambda_{max} = 4.90 \text{ m}$$

Length of the resonance tube and the frequency range

As the maximum possible tube length of 4.90 m is not suitable for interferometric measurements, the following dimensions of the tube length are selected for our measurements

$$0.5334 \text{ m} \leq l \leq 0.9144 \text{ m}.$$

Hence, the range of operating frequencies is

$$187 \text{ Hz} \leq f \leq 321 \text{ Hz}.$$

3.4. Optimum stack position and expected temperature differences

Theory

Atchley *et al.* (1990) have conducted a thorough, quantitative investigation of the basic theory underlying thermoacoustic heat transport for the simplest class of thermoacoustic engine, a stack of short plates referred to as a thermoacoustic couple (TAC). They measured the temperature difference developed across the short stack of plates in acoustic standing waves as a function of the position of the plates in the acoustic field, drive ratio, plate configuration, thermal properties of the plates, and thermophysical properties of the gas. The temperature differences between the two ends of the stack plates are due to the net effect of the shuttling action of the gas parcels by removing heat from one side and accumulating the heat at the other. In other words, the end of the plate closer to the pressure node gets cooler and the side of the stack closer to the pressure antinode gets warmer and there is no net heat loss or gain by interior portions of the plates.

The equation for the theoretical temperature gradient

The following equation for the steady-state temperature difference developed across a TAC in an acoustic standing wave was originally derived by Wheatly *et al.* (1983) and slightly altered by Atchley *et al.* (1990) to include the effect of thermal conduction through the gas:

$$\Delta T = \frac{\sqrt{\frac{K_g}{\rho_m c_p \pi \frac{c}{\lambda}}} \frac{P_0^2(1+\sqrt{\sigma})}{4\rho_m c(K_p d_p + K_g d_g)(1+\sigma)} * \Delta x * \sin(4\pi\lambda^{-1}x)}{1+\sqrt{\frac{K_g}{\rho_m c_p \pi \frac{c}{\lambda}}} \frac{P_0^2(1-\sigma\sqrt{\sigma})}{4(K_p d_p + K_g d_g)\rho_m T_m 2\pi \frac{c}{\lambda}(\gamma-1)(1-\sigma^2)} [1-\cos(4\pi\lambda^{-1}x)]}$$

For this equation it is assumed that $\Delta x << \lambda/2\pi$; δ_κ , $\delta_\nu << d_g$; and $\Delta T << T_m$ and that the presence of the stack does not significantly influence the acoustic standing wave. Furthermore, the heat capacity of the plate is considered much greater than that of the gas, so that the temperature of the plate surface does not oscillate on an acoustic time scale.

In order to estimate a suitable stack length and stack position as well as to calculate the temperature difference corresponding to different stack length and stack positions following variables and parameters are determined:

a) Variables

ΔT	temperature difference	°C	result
Δx	stack length	m	0.01 - 0.10 m
x	position of center point of stack from rigid wall	m	0 - 0.0254 · l
P_0	dynamic pressure amplitude	Pa	0.5% - 3 %
l	tube length	inch	21 to 36
T_m	mean temperature	K	273 K; 293 K

b)	Constants		
c	speed of sound in air	m/s	depends on T_m
c_p	isobaric heat capacity per unit mass for air	kg/m^3	1006
d_g	plate separation	m	0.005
d_p	plate thickness	m	0.001
λ	wavelength	m	$0.0508 \cdot l$
γ	ratio of specific heats of air	-	1.40
k_g	thermal conductivity of air	W/m· K	depends on T_m
k_p	thermal conductivity of plate (acrylglass)	W/m· K	0.184
ρ_m	mean air density	kg/m^3	depends on T_m
σ	Prandtl number of air	-	0.72

Temperature differences for different stack lengths

Figure 2 presents graphically the result of the calculation of the theoretical temperature differences by varying the stack lengths between 0.01m and 0.1m, at a frequency of 321 Hz and corresponding tube length of 0.5334 m. The operating temperature selected for the calculations is 293 K, which means that the speed of sound in air is c = 342.9 m/s, the thermal conductivity of air is k_g = 0.0257 W/mK, and the mean density of air is ρ_m = 1.205 kg/m^3. The maximum dynamic pressure amplitude is considered to be 3% of the mean atmospheric pressure.

The calculations indicated that by increasing the stack length the theoretical temperature difference increases as well. In order to satisfy both, a maximum theoretical temperature difference and the requirements for the interferometric measurement technique, the stack length is determined to 0.0762m.

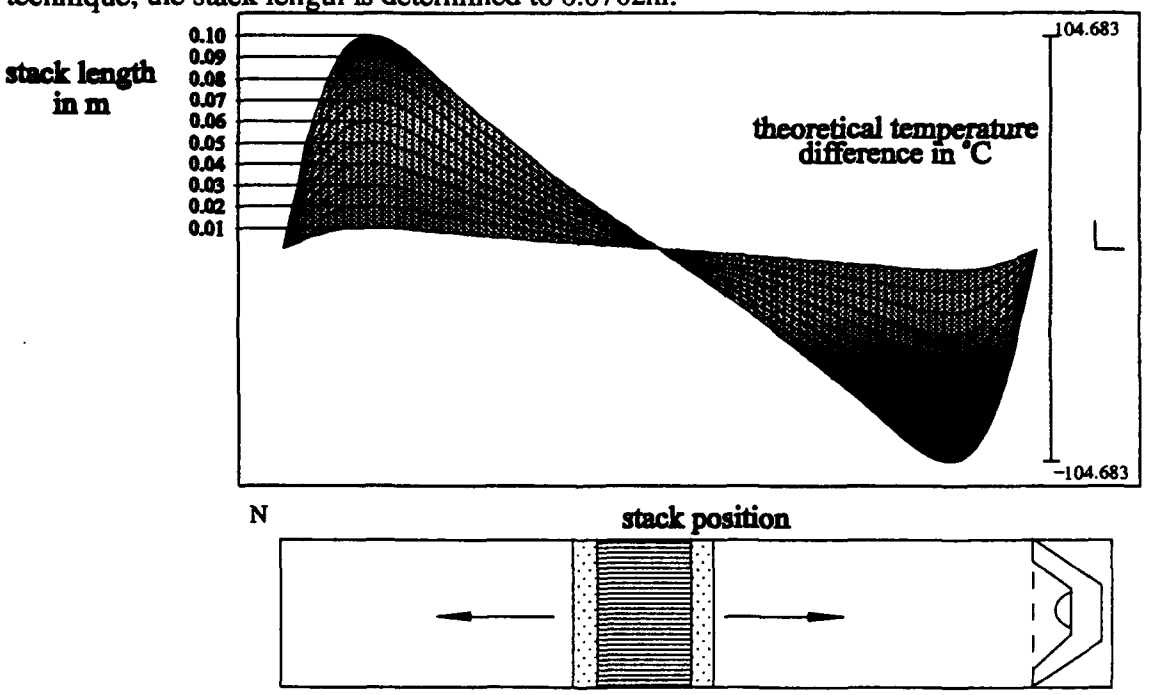

Figure 2: Theoretical temperature difference by varying the stack length and stack position within the resonance tube

Determination of the exact stack position

The optimum position of the stack should be a compromise to match the requirements regarding different temperatures, pressure amplitudes, tube lengths and frequencies. In order to satisfy these requirements several cases, applying the equation mentioned above, are calculated. The best compromise could be achieved by a stack center position of 0.127 m from the loudspeaker membrane, which ensures high enough temperature differences between the ends of the stack plates.

4. INSTRUMENTATION

Acoustic power delivered by the loudspeaker

For calculations of the acoustic power, the knowledge of the oscillation amplitude of the loudspeaker membrane is essential. The minimum amplitude is obviously 0 mm, and the maximum amplitude, indicated by the loudspeaker manufacturer, is 6 mm. For the estimation of the theoretical acoustic power input to the resonance tube, the appropriate working range for the membrane amplitude was selected as:

amplitude: $A_{min} = 1.0$ mm and $A_{max} = 4.0$ mm,

and the limiting frequencies are

minimum frequency $f_{min} = 187$ Hz

maximum frequency $f_{max} = 321$ Hz

With the following equations

- $s(t) = A \sin(\omega t)$
- $v(t) = A\,\omega \cos(\omega t)$
- $a(t) = -A\,\omega^2 \sin(\omega t)$ and: $\omega = \text{constant} = 2\pi f$

with: A - amplitude

ω - angular frequency

both velocity and acceleration of the loudspeaker membrane can be calculated.

Velocity of the loudspeaker membrane

The maximum value for the velocity, v_{max}, is determined from the condition $\cos(\omega t) = 1$. Hence, the time t is:

$$t = \frac{n}{2} T \qquad \text{with: } n = 1,2,3,.....$$

Thus, the maximum velocity of the loudspeaker membrane will be:

$$v_{max} = A\,\omega = 2\,A\,\pi\,f,$$

which leads to the following results for the maximum velocity for the given ranges of frequencies and amplitudes:

$\Rightarrow 1.175 \frac{m}{s} \le v_{max} \le 4.70 \frac{m}{s}$ for $f = 187$ Hz and $0.001 \text{ m} \le A \le 0.004$ m

$\Rightarrow 2.017 \frac{m}{s} \le v_{max} \le 8.06 \frac{m}{s}$ for $f = 321$ Hz and $0.001 \text{ m} \le A \le 0.004$ m

Acceleration of the loudspeaker membrane

In order to obtain the maximum value for the acceleration of the loudspeaker membrane a_{max}, the condition $\sin(\omega t) = 1$ has to be satisfied. Hence the time t is

$$t = \frac{2n - 1}{4} T \qquad \text{with } n = 1,2,3,.....$$

The maximum acceleration will be

$$a_{max} = A\ \omega^2 = 4\ A\ \pi^2 f^2$$

$$\Rightarrow 1380\ \tfrac{m}{s^2} \le a_{max} \le 5522\ \tfrac{m}{s^2} \quad \text{for } f = 187 \text{ Hz and } 1.0 \text{ mm} \le A \le 4.0 \text{ mm}$$

$$\Rightarrow 4068\ \tfrac{m}{s^2} \le a_{max} \le 16271\ \tfrac{m}{s^2} \quad \text{for } f = 321 \text{ Hz and } 1.0 \text{ mm} \le A \le 4.0 \text{ mm}$$

Acoustic energy generated by the loudspeaker

The acoustic energy that can be theoretically radiated into the tube of the thermoacoustic heat pump model is calculated as

$$P_R = \tfrac{1}{2}\ \pi r^2 \rho c R_1 U^2,$$

with

$$R_1 = \frac{(2kr)^2}{8}.$$

The values used in the calculations are the following:

radius of the loudspeaker membrane	$r = 0.076$ m
characteristic impedance of air [5]	$\rho c = 414.0\ \frac{Kg}{m^2 s}$
speed of sound	$c = 343.11\ \frac{m}{s}$
range of frequencies:	$187 \text{ Hz} \le f \le 321 \text{ Hz}$

Hence:

- range of variable R_1 with $k = \frac{\omega}{c}$: $0.03386674 \le R_1 \le 0.099793$
- range of membrane velocities: $1.175\ \frac{m}{s} \le U \le 8.06\ \frac{m}{s}$

For these values the power of the sound emitted by the membrane is

$$0.176 \le P_R \le 24.35 \text{ W}$$

Expected pressure amplitudes

The next step in the calculation is to estimate the pressure amplitude that can be delivered from the membrane of the loudspeaker. The pressure can be determined as

$$p = v\ \rho\ c$$

with:

p	- pressure difference relative to atmospheric pressure
v	- membrane velocity and
ρc	- characteristic impedance of air

As the most important values for this calculation are the minimum and maximum membrane velocities, $v_{min} = 1.175\ \frac{m}{s}$ and $v_{max} = 8.06\ \frac{m}{s}$. The pressure amplitude to be expected is in the following range:

$$486 \text{ Pa} \le p \le 3337 \text{ Pa}$$

The dynamic pressure is then in a range of

$$0.48\% \text{ - } 3.3\%$$

relative to the atmospheric pressure of $p_m = 101325$ Pa. These calculations indicate that the selected loudspeaker is capable of delivering sufficient acoustic energy to drive the thermoacoustic heat pump model.

Measurement of acoustic energy

The pressure transducer. In order to calculate the actual acoustic power input during the operation of the heat pump, information on the dynamic pressure amplitude is required. Pressure transducers use sensor chips or fragile membranes to measure pressure. Differential pressure transducers measure the difference between two pressure sources. The pressure difference is then obtained by pointing one side of the device membrane to one pressure source and leaving the other port open to the atmosphere. As the maximum change of the dynamic pressure is about 3% of the atmospheric pressure, a gage pressure transducer is the obvious choice.

One pressure transducer that fulfills the requirements regarding accuracy, cost, low noise, air flow monitoring and low power consumption is the SX01D pressure transducer from SenSym. This transducer is operating in a differential pressure range between 0 and 1 psi. This matches well the operating pressure range of the heat pump.

The accelerometer. In order to determine the sound power emitted by the acoustic driver during the operation of the heat pump, the velocity of the loudspeaker membrane must be measured. As the velocity cannot be measured directly, an accelerometer will be used, and the acceleration signal will be integrated into velocity. An important requirement is a low mass of the transducer, in order to avoid influencing the membrane mass.

The accelerometer chosen for the present application is the EGA-125-2500 Miniature Accelerometer from Entran. Its weight without wiring is 0.5 grams, it has an acceleration range of ± 2500g with a sensitivity of 0.069 mV/g and can be used up to a frequency of 1800 Hz. These specifications exactly match all the requirements for our application. The semiconductor circuitry of the transducer is fully compensated for temperature changes within a range from 21° to 77°C.

The power supply. In order to drive both the pressure transducer and the accelerometer, the PS-15 power supply by Entran was selected. It has an adjustable sensor excitation from 1 to 15 VDC, and can be used for both transducers. The power supply generates a DC supply voltage of high stability and low noise. The signal output port of the power supply will mainly be used for the accelerometer, whereas the signal output from the pressure transducer will be connected to an amplifier or a data acquisition board.

5. ACCOMPLISHMENTS

During the past project period, the thermoacoustic device model was built, measurement tasks were identified, and sensors necessary for the measurements were selected and purchased. A photograph of the thermoacoustic device model and instrumentation is presented in Figure 3.

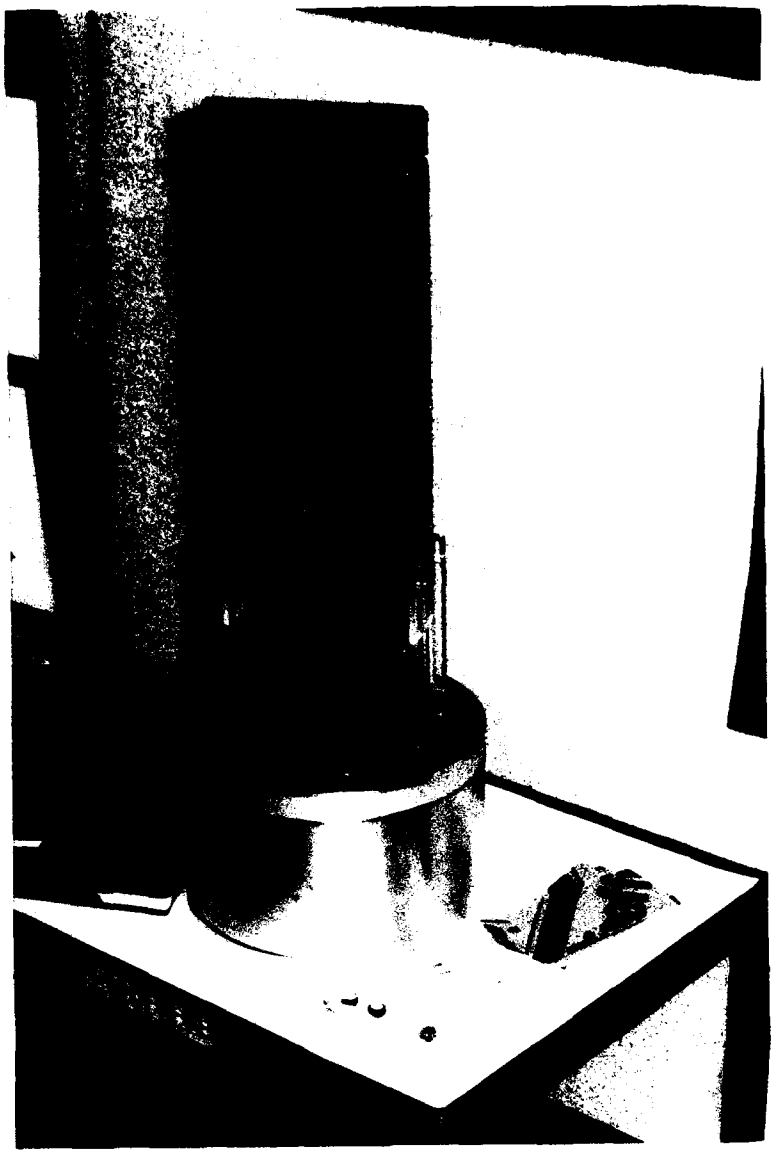

Figure 3. Thermoacoustic device model and instrumentation

6. FUTURE PLANS

Experiments with the thermoacoustic device model:

1. Basic power, pressure and temperature measurements.
2. Visualization of temperature fields by holographic interferometry and heat transfer measurements.
3. Flow visualization by smoke injection.
4. Measurement of the temperature distribution in the stack plates using thermochromatic liquid crystals.
5. Evaluation of the visualization measurements.
6. Design of the heat exchangers.
7. Investigation of the operating mode as prime mover.

PERSONNEL

1. Cila Herman, Assistant Professor
2. Christoph Bartscher, Visiting Scholar

REFERENCES

1 Leo L. Beranek, "Acoustics", Published for the Acoustical Society of America by the American Institute of Physics, (1990)

2 Joseph L. Hunter, "Acoustics", Prentice-Hall, Inc., Sept. 1965

3 Atchley A.A., Hofler T.J., Muzzeral M.L., Kite M.D., Ao C., "Acoustically generated temperature gradients in short plates", J. Acoust. Soc. Am. 88 (1), July 1990

4 J. Wheatley, T. Hofler, G.W. Swift, A. Migliory, " An instrinsically irreversible thermoacoustic heat engine", J. Acoust.Soc.Am. 74 (1), July 1983

5 E. Meyer, E.-G. Neumann, "Physical and applied acoustics", Academic Press, New York, (1972)

O.M. Knio and A. Worlikar

NUMERICAL MODELING EFFORT

OBJECTIVES

The objective of this phase of the effort is the development of a computational methodology for simulation of the flow in the neighborhood of a thermoacoustic stack, and the implementation of the numerical schemes to analyze flowfield response to different acoustic forcing levels.

This effort complements ongoing experimental and theoretical efforts aiming at an improved fundamental understanding of thermoacoustic devices. The development of these parallel efforts is described separately. This section thus provides a summary of numerical modeling activities.

APPROACH

In its simplest form, a thermoacoustic devices consists of a straight resonance tube and a stack of parallel plates. The arrangement is schematically illustrated in Fig. 1. By exciting a standing wave within the resonance tube, it is now well-established that a temperature gradient develops across the stack, thereby enabling heat exchange between a two systems or between a system and a reservoir.

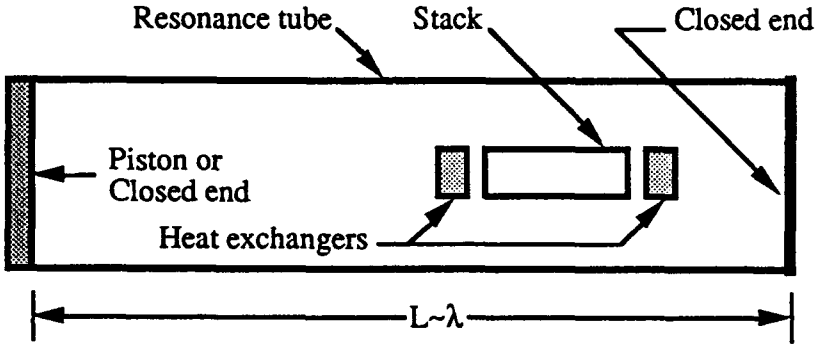

Figure 1. Schematic illustration of a thermoacoustic device.

As mentioned above, simulation of the flowfield in a small neighborhood of the stack is targeted. Since the length of the stack, L, is typically much smaller than that of the resonance tube, A, it is highly desirable to adopt a simplified flow model which enables us to isolate the stack, while at the same time retaining all of the essential features of the entire system. To this end, we first adapt a simplified low-Mach-number compressible model which meets this requirement.

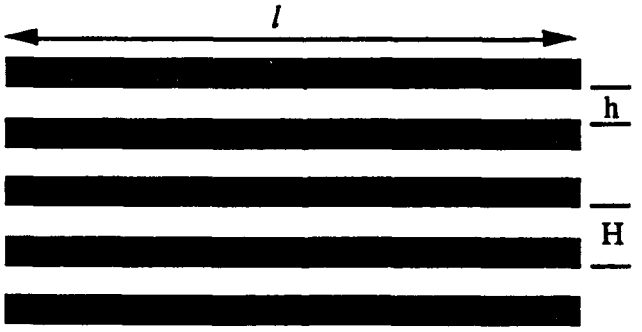

Figure 2. Schematic illustration of a thermoacoustic stack consisting of thin closely spaced flat plates.

The basic assumptions used in the construction of the model are: (1) the length of the stack is much shorter than that of the resonance tube so that, in a small neighborhood of the stack, the low-Mach-number limit of the compressible momentum and energy equations can be adopted; (2) away from the stack, the flowfield is assumed to be well approximated by an idealized acoustic standing wave. These assumptions enable us to follow a construction that is similar to that used in the development of a large number of reacting flow models, *e.g.* [1-4]. We start from the governing equations for compressible non-reacting flow of an ideal gas (Table 1), normalized with respect to appropriate characteristic length, velocity, density and pressure scales.

TABLE 1
Governing Equations for Compressible Fluid Flow

Mass
$$\frac{D\rho}{Dt} + \rho \nabla \bullet \mathbf{u} = 0 \tag{1.1}$$

Momentum
$$\gamma M^2 \rho \frac{D\mathbf{u}}{Dt} = -\nabla p + \frac{\gamma M^2}{\mathrm{Re}} \nabla \bullet \tau \tag{1.2}$$

Energy
$$\rho \frac{DT}{Dt} - \frac{\gamma - 1}{\gamma} \frac{Dp}{Dt} = -\frac{1}{Pe} \nabla \bullet \mathbf{q} + \frac{(\gamma - 1) M^2}{\mathrm{Re}} \varphi \tag{1.3}$$

State
$$p = \rho T \tag{1.4}$$

Next, we expand all relevant quantities in terms of powers of $\varepsilon \equiv \gamma M^2$, where γ is the specific heat ratio and M is the Mach number, *i.e.* by expressing a generic gasdynamic variable $\varsigma(\mathbf{x},t)$ in series form as:

$$\varsigma(\mathbf{x},t) = \varsigma_o(\mathbf{x},t) + \varepsilon \varsigma_1(\mathbf{x},t) + \varepsilon^2 \varsigma_2(\mathbf{x},t) + \cdots \tag{1}$$

Substituting the appropriate expansions into the momentum equations, and collecting the zeroth power in ε, immediately yields:

$$\nabla p_o = 0 \tag{2}$$

i.e. the zeroth component of pressure is spatially uniform, and therefore a function of time only. By an abuse of terminology and notation, we shall call this pressure component the thermodynamic pressure and denote it by $P(t)$. To first order in ε, one has:

Momentum (ε):
$$\rho_o \frac{D\mathbf{u}_o}{Dt} = -\nabla p_1 + \frac{1}{\mathrm{Re}} \nabla \bullet \tau \tag{3}$$

Energy (ε):
$$\rho_o \frac{DT_o}{Dt} - \frac{\gamma - 1}{\gamma} \frac{dP}{dt} = \frac{1}{Pe} \nabla^2 T \tag{4}$$

Note that the energy balance is independent of p_1 and that viscous dissipation has been neglected. A more convenient form of the energy equation is obtained by differentiating the (zeroth order) equation of state:

$$\frac{dP}{dt} = \rho_o \frac{DT_o}{Dt} + T_o \frac{D\rho_o}{Dt} \tag{5}$$

and combining with the continuity equation to get:

$$\nabla \bullet \mathbf{u}_o = -\frac{1}{\gamma P} \frac{dP}{dt} + \frac{1}{P} \frac{1}{Pe} \nabla^2 T \tag{6}$$

In the geometry considered, velocity fluxes into the system are known, following the assumption that matching with an idealized sound wave away from a stack occurs. This enables us to integrate the above equation over the entire volume of the computational domain to get:

$$\frac{V}{\gamma} \frac{dP}{dt} = -P \int \mathbf{u}_o \bullet \mathbf{n} \, dA + \frac{1}{Pe} \int \nabla T \bullet \mathbf{n} \, dA \tag{7}$$

Next, we adopt a vorticity-based formulation of the equations of motion. The derivation relies on the Helmholtz decomposition of the velocity field into divergence-free and irrotational components, and on the vorticity form of the momentum equation. Thus, we first let:

$$\mathbf{u}_o = \nabla \phi + \mathbf{u}_\omega \tag{8}$$

where ϕ is a potential function and $\mathbf{u}_\omega$ is the divergence-free vortical velocity component. Substituting Eq. (8) into Eq. (6), one gets:

$$\nabla^2\phi = \frac{1}{P}\left[-\frac{1}{\gamma}\frac{dP}{dt} + \frac{1}{Pe}\nabla^2 T\right] \tag{9}$$

Second, taking the curl of the momentum equations, we have:

$$\frac{\partial\omega}{\partial t} + \nabla\times(\omega\times\mathbf{u}) = -\frac{\nabla\rho_o}{\rho_o}\times\frac{D\mathbf{u}}{Dt} + \frac{1}{\rho_o \mathrm{Re}}\nabla\times(\nabla\bullet\tau) \tag{10}$$

For constant viscosity, the divergence of the dimensional viscous stress tensor can be written as:

$$\nabla\bullet\tilde{\tau} = -\tilde{\mu}\nabla\times\tilde{\omega} + \tilde{\lambda}\nabla\bullet\tilde{\mathbf{u}} \tag{11}$$

so that

$$\begin{aligned}\nabla\times(\nabla\bullet\tilde{\tau}) &= -\tilde{\mu}\nabla\times(\nabla\times\tilde{\omega})\\ &= \tilde{\mu}\nabla^2\tilde{\omega}\end{aligned} \tag{12}$$

It follows that Eq. (10) can be rewritten as:

$$\frac{\partial\omega}{\partial t} + \nabla\times(\omega\times\mathbf{u}) = -\frac{\nabla\rho_o}{\rho_o}\times\frac{D\mathbf{u}}{Dt} + \frac{1}{\rho_o \mathrm{Re}}\nabla^2\omega \tag{13}$$

The derivation of Eq. (13) completes the construction of the physical model; a summary of the governing equations in given in Table 2. For clarity and convenience, the subscripts o,1 are omitted from Table 2; this simplified convention will also be adopted in the remainder of this manuscript.

Table 2
Summary of Model Equations

Helmholtz Decomposition:

$$\begin{cases}\mathbf{u} = \nabla\phi + \nabla\times\psi\\ \nabla^2\psi = -\omega\end{cases} \tag{2.1}$$

Continuity:

$$\begin{cases} \nabla^2\phi = \dfrac{1}{P}\left[-\dfrac{1}{\gamma}\dfrac{dP}{dt} + \dfrac{1}{Pe}\nabla^2 T\right] \\ \dfrac{V}{\gamma}\dfrac{dP}{dt} = -P\int \mathbf{u}\bullet\mathbf{n}\, dA + \dfrac{1}{Pe}\int \nabla T\bullet\mathbf{n}\, dA \end{cases} \tag{2.2}$$

State:

$$p = \rho T \tag{2.3}$$

Energy:

$$\rho\frac{DT}{Dt} - \frac{\gamma-1}{\gamma}\frac{dP}{dt} = \frac{1}{Pe}\nabla^2 T \tag{2.4}$$

Vorticity Transport:

$$\frac{\partial\omega}{\partial t} + \nabla\times(\omega\times\mathbf{u}) = -\frac{\nabla\rho}{\rho}\times\frac{D\mathbf{u}}{Dt} + \frac{1}{\rho\,\mathrm{Re}}\nabla^2\omega \tag{2.5}$$

Normalization

Despite the relative simplicity of the geometry of the thermoacoustic stack, there exists a multitude of appropriate conventions which can be adopted in the normalization of the governing equations. Thus, it is worthwhile providing clear descriptions of normalizing parameters, and of the meaning of the resulting dimensionless groups. Below, we shall choose the plate separation distance, $\tilde{H}$, as reference lengthscale and the quantity $\tilde{\Omega}\tilde{H}$ as reference velocity scale. This convention naturally leads to the following definition of the Reynolds number:

$$\mathrm{Re}_\delta \equiv \frac{\tilde{\Omega}\tilde{H}^2}{\tilde{\nu}} \tag{14}$$

We shall refer to Re_δ as the "Stokes layer Reynolds number" since it effectively relates the thickness of the Stokes layer,

$$\tilde{\delta} \approx 6.4\sqrt{\frac{\tilde{\nu}}{\tilde{\Omega}}} \tag{15}$$

to the plate spacing, $\tilde{H}$, through:

$$\frac{\tilde{\delta}}{\tilde{H}} \approx \frac{6.4}{\sqrt{\mathrm{Re}_\delta}} \tag{16}$$

Other useful conventions for the Reynolds number include: (a) the "acoustic amplitude Reynolds number",

$$\mathrm{Re}_a \equiv \frac{2\tilde{a}}{\sqrt{\tilde{\nu}\tilde{\Omega}}} \tag{17}$$

which is a dynamic Reynolds number based on the acoustic wave's velocity amplitude, $\tilde{a}$, the thickness of the Stokes layer, and the kinematic viscosity; and (b) the "particle displacement Reynolds number,"

$$\mathrm{Re}_p \equiv \frac{\tilde{a}}{\tilde{\Omega}\tilde{H}} \tag{18}$$

which characterizes the ratio of a characteristic particle displacement during a wave cycle to the plate separation distance. It is interesting to note that these three Reynolds numbers are related through: $\mathrm{Re}_a^2 / \mathrm{Re}_\delta \equiv 4\mathrm{Re}_p^2$.

Following the above discussion, the physical operating conditions of a thermoacoustic stack are determined in terms of the following set of dimensionless parameters: (a) one kinematic Reynolds number, *i.e.* Re_δ or Re_p; (b) the dynamic Reynolds number, Re_a or, equivalently, the acoustic drive ratio, R, (c) either the Prandtl number, Pr, or the Peclet number, Pe; (d) a plate thickness parameter, *e.g.* the channel width to plate spacing ratio, $\tilde{h} / \tilde{H}$; (e) a plate length parameter, *e.g.* the plate length to spacing ratio, $\tilde{l} / \tilde{H}$; and (f) the location of the thermoacoustic stack with respect to the driving acoustic wave, *e.g.* in terms of a dimensionless wavenumber $\tilde{\kappa}\tilde{x}$. Thus, even if the above simplified model is adopted, a high-dimensional parameter space is still needed to describe the relevant dynamics.

Computational Methodology

Simulation of the governing model equations is performed using a finite difference methodology. To this end, the computational domain is divided using a square rectangular grid with mesh size $\Delta x = \Delta y$ (Fig. 3). All spatial derivatives are discretized using the standard second-order centered differences, while time derivatives are treated using the third-order Adams-Bashforth integration scheme.

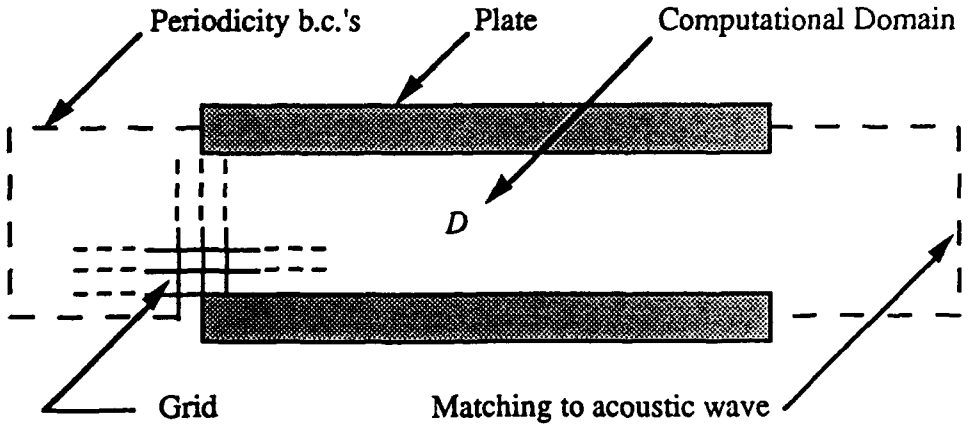

Figure 3. Schematic illustration of the computational domain.

Assuming all the relevant quantities known at time $t = n\Delta t$, the solution is advanced in time as summarized below:

(a) Integrate numerically Eq. (2.2b) in order to determine the thermodynamic pressure at the new time step:

$$\frac{P^{n+1} - P^n}{\Delta t} = -\frac{\gamma}{V}\sum_{j=0}^{2}\beta_j\left[P^{n-j}\int \mathbf{u}_a^{n-j}\bullet\mathbf{n}\,dA + \frac{1}{Pe}\int \nabla_h T^{n-j}\bullet\mathbf{n}\,dA\right] \tag{19}$$

(b) Integrate the energy equation in order to determine the new temperature distribution within the domain:

$$\frac{T^{n+1} - T^n}{\Delta t} = \sum_{j=0}^{2}\beta_j\left[-\frac{\mathbf{u}^{n-j}\bullet\nabla_h T^{n-j}}{\rho^{n-j}} + \frac{\gamma-1}{\gamma\rho^{n-j}}\frac{dP^{n-j}}{dt} + \frac{1}{Pe}\nabla_h^2 T^{n-j}\right] \tag{20}$$

(c) Using the equation of state, Eq. (2.3), determine the new value of the density distribution:

$$\rho^{n+1} = \frac{P^{n+1}}{T^{n+1}} \tag{21}$$

(d) Based on the new values of pressure, temperature and density, compute the new rate of pressure change using Eq. (2.2b):

$$\frac{dP^{n+1}}{dt} = \frac{\gamma}{V}\left[-P^{n+1}\int \mathbf{u}_a^{n+1}\bullet\mathbf{n}\,dA + \frac{1}{Pe}\int \nabla_h T^{n+1}\bullet\mathbf{n}\,dA\right] \tag{22}$$

(e) Solve the following Neumann problem to determine the new potential distribution with the computational domain:

$$\begin{cases} \nabla_h^2\phi^{n+1} = \dfrac{1}{P^{n+1}}\left[-\dfrac{1}{\gamma}\dfrac{dP^{n+1}}{dt} - \dfrac{1}{Pe}\nabla_h^2 T^{n+1}\right] & \\ \dfrac{\partial\phi}{\partial n}^{n+1} = 0 & \text{on solid surfaces} \\ \dfrac{\partial\phi}{\partial n}^{n+1} = u_a^{n+1} & \text{on matching surfaces} \end{cases} \tag{23}$$

(f) Integrate the vorticity transport equation in order to determine the new vorticity distribution in the interior of the computational domain:

$$\frac{\omega^{n+1} - \omega^n}{\Delta t} = \sum_{j=0}^{2}\beta_j\left[\nabla_h\times\left(\mathbf{u}^{n-j}\times\omega^{n-j}\right) - \frac{\nabla_h\rho^{n-j}}{\rho^{n-j}}\times\frac{D\mathbf{u}^{n-j}}{Dt} + \frac{1}{\rho^{n-j}\,\mathrm{Re}}\nabla_h^2\omega^{n-j}\right] \tag{24}$$

(g) Determine the new streamfunction distribution within the computational domain and the vorticity distribution along solid boundaries:

$$\begin{cases} \nabla_h^2 \psi^{n+1} = -\omega^{n+1} & \\ \psi^{n+1} = 0 & \text{on all boundaries} \end{cases} \tag{25}$$

ACCOMPLISHMENTS

Numerical modelling activities conducted during the first phase of this collaborative research effort resulted in:

(1) development of the simplified physical model equations summarized above;

(2) formulation of a computational methodology for the simulation of the governing equations; and,

(3) construction of computer codes reflecting the results of (1-2) above, and vectorization and optimization of one version of the code for the CRAY-C90 at the Pittsburgh Supercomputer Center.

Implementation of the numerical schemes have so far focused on a visualization of the flowfield in the neighborhood of the thermoacoustic stack. Samples of computations performed are presented as Figs. 4-6, which depict instantaneous streamfunction distributions for different stack locations within the resonance tube. Detailed analysis of the results of these computations will be given elsewhere [5].

Future plans include:

(1) application of the computational schemes to analyze the impact of non-linear dynamics on flowfield behavior ;

(2) analysis of computed results in order to evaluate one-dimensional theories and to derive, if necessary, corrections to these theories in order to account for neglected dynamics;

(3) extension of the physical model and of the computational schemes in order to (i) account for heating loads, and (ii) accommodate a more detailed coupling between flowfield dynamics in the neighborhood of the stack and the driving acoustic wave; and,

(4) validation of the numerical schemes by comparing computed predictions with experimental results; and,

(5) implementation of the validated schemes to characterize the performance of thermoacoustic refrigerators under a wide range of operating conditions.

PERSONNEL

1. Omar M. Knio, Assistant Professor
Department of Mechanical Engineering
The Johns Hopkins University
Baltimore, MD 21218-2686

2. Aniruddha Worlikar, Graduate Research Assistant
Department of Mechanical Engineering
The Johns Hopkins University
Baltimore, MD 21218-2686

REFERENCES

1. Majda, A. and Sethian, J., *Combust. Sci. and Tech.* **42**, 185, 1985.
2. Ghoniem, A.F. and Knio, O.M. in *Twenty First Symposium (International) on Combustion*, p. 1313, The Combustion Institute, 1986.
3. Ghoniem, A.F., in *Lectures in Applied Mathematics* **24**, p. 199, 1985.
4. McMurtry, P.A., Jou, W.-H., Riley, J.J. and Metcalfe, R.W. *AIAA J.* **24**, p. 962, 1986.
5. A. Worlikar & O.M. Knio, "Numerical Study of Unsteady Flow in the Neighborhood of a Thermoacoustic Stack," *in preparation.*
6. A.A. Atchley, T.J. Hofler, M.L. Muzzerall, M.D. Kite & C. Ao, *J. Acoust. Soc. Am.* **88**, p. 251, 1990.

NOMENCLATURE

Roman

a	acoustic wave velocity amplitude
A	surface
c	sound speed
c_p	specific heat at constant pressure
D	computational domain
$\frac{D}{Dt} \equiv \frac{\partial}{\partial t} + \mathbf{u} \bullet \nabla$	material derivative
h	channel height
H	plate spacing
k	thermal conductivity
l	plate length
L	length of computational domain
M	Mach number
$\mathbf{n}$	outer normal
p	pressure
P	thermodynamic pressure
$Pe \equiv \tilde{\Omega}\tilde{H}^2 / \tilde{\alpha}$	Peclet number
$\mathrm{Pr} \equiv \tilde{\nu} / \tilde{\alpha}$	Prandtl number
$\mathbf{q} \equiv -k\nabla T$	conduction heat flux
R	drive ratio
$\mathrm{Re}_a \equiv 2\tilde{a} / \sqrt{\tilde{\nu}\tilde{\Omega}}$	acoustic amplitude Reynolds number
$\mathrm{Re}_\delta \equiv \tilde{\Omega}\tilde{H}^2 / \tilde{\nu}$	Stokes layer Reynolds number
$\mathrm{Re}_p \equiv \tilde{a} / \tilde{\Omega}\tilde{H}$	particle displacement Reynolds number
t	time
$\mathbf{u} = (u, v)$	flow velocity
V	volume

Greek

$\alpha = k / \rho c_p$	thermal diffusivity
β	constant
γ	specific heat ratio
δ	thickness of the Stokes layer
ϕ	velocity potential
φ	viscous dissipation function
$\kappa \equiv \Omega / c$	wavenumber
λ	second coefficient of viscosity
μ	dynamic viscosity
ν	kinematic viscosity
ρ	density
$\tilde{\tau}$	shear stress tensor
ω	vorticity
ψ	streamfunction
$\Delta x, \Delta y$	grid size
Ω	angular frequency

Subscripts

ω	vortical component
o,1	zeroth or first order
a	acoustic
h	discrete

Superscripts

~	dimensional quantity
n	time level

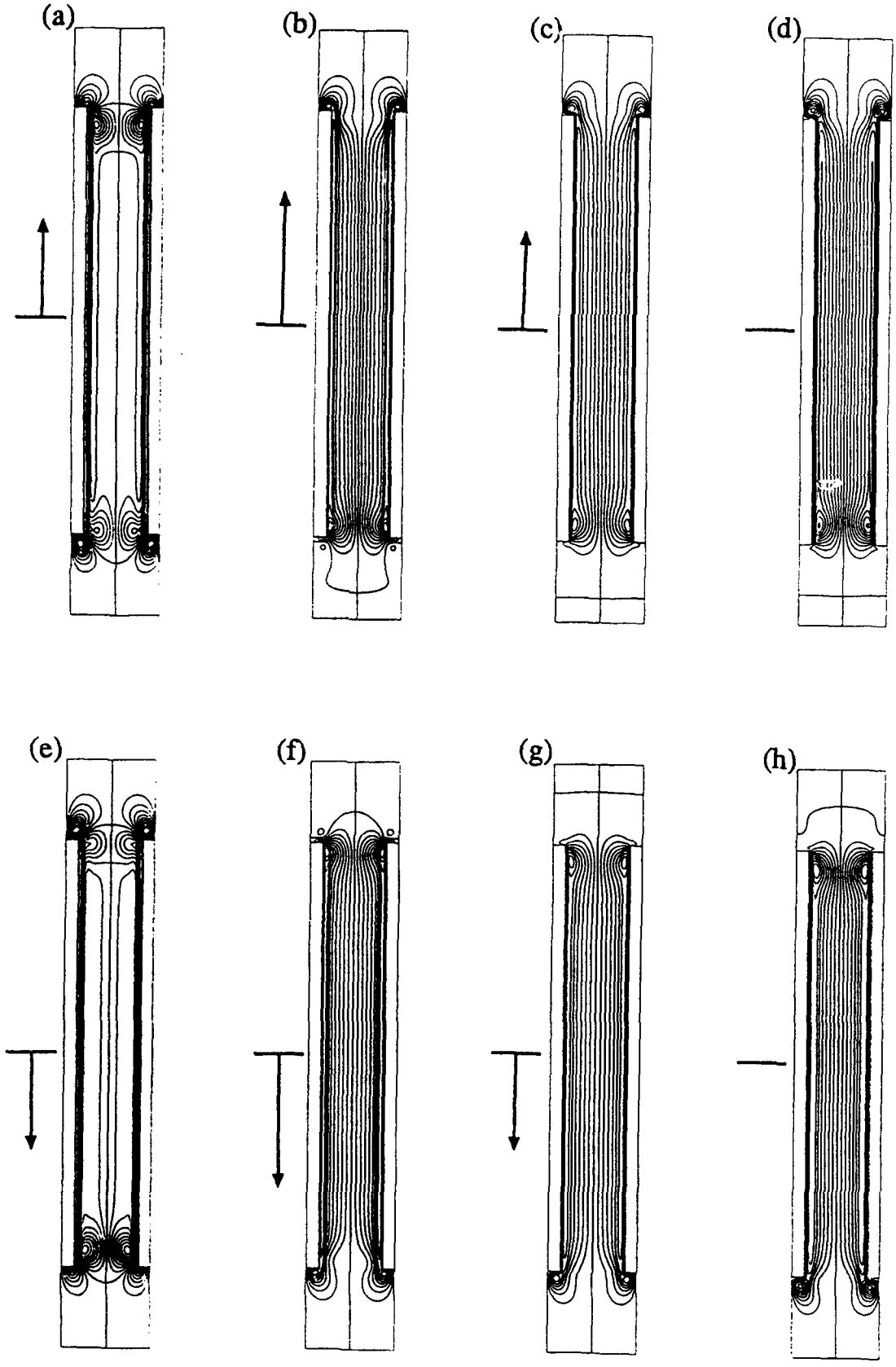

FIG 4: Instantaneous streamfunction distribution in the neighbourhood of a thermoacoustic stack at (a) $\theta = 19.634$,(b) $\theta = 20.42$, (c) $\theta = 21.205$, (d) $\theta = 21.99$, (e) $\theta = 22.77$, (f) $\theta = 23.56$, (g) $\theta = 24.34$, (h) $\theta = 25.132$. The stack has the same dimensions as stack no 1. as used by Atchley [6], (L/H = 4.727 h/H=0.727) and is located at $\tilde{k}\tilde{x}=\pi/2$. The drive ratio R= 0.13%; $Re_a = 0.8879$; $Re_p = 0.0096$; $Re_\delta = 2132$. The arrows indicate the magnitude and the direction of the acoustic velocity at the center of the stack.

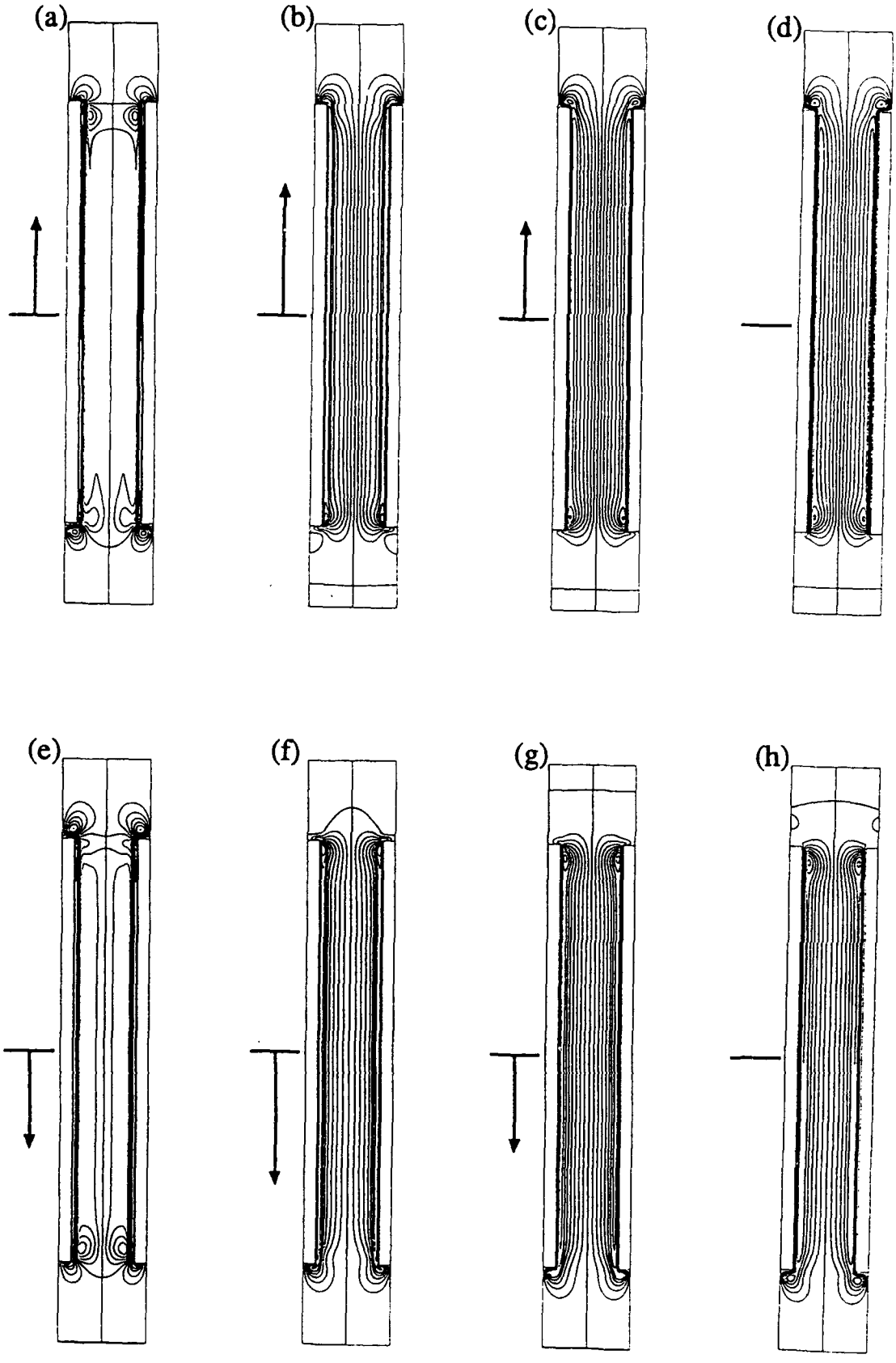

FIG 5: Instantaneous streamfunction distribution in the neighbourhood of a thermoacoustic stack at (a) $\theta = 19.634$,(b) $\theta = 20.42$, (c) $\theta = 21.205$, (d) $\theta = 21.99$, (e) $\theta = 22.77$, (f) $\theta = 23.56$, (g) $\theta = 24.34$, (h) $\theta = 25.132$. The stack has the same dimensions as stack no 1. as used by Atchley [6], (L/H = 4.727 h/H=0.727) and is located at $\tilde{k}\tilde{x}=3\pi/4$. The drive ratio R= 0.13% ; $Re_a = 0.8879$ $Re_p = 0.0096$; $Re_\delta = 2132$. The arrows indicate the magnitude and the direction of the acoustic velocity at the center of the stack

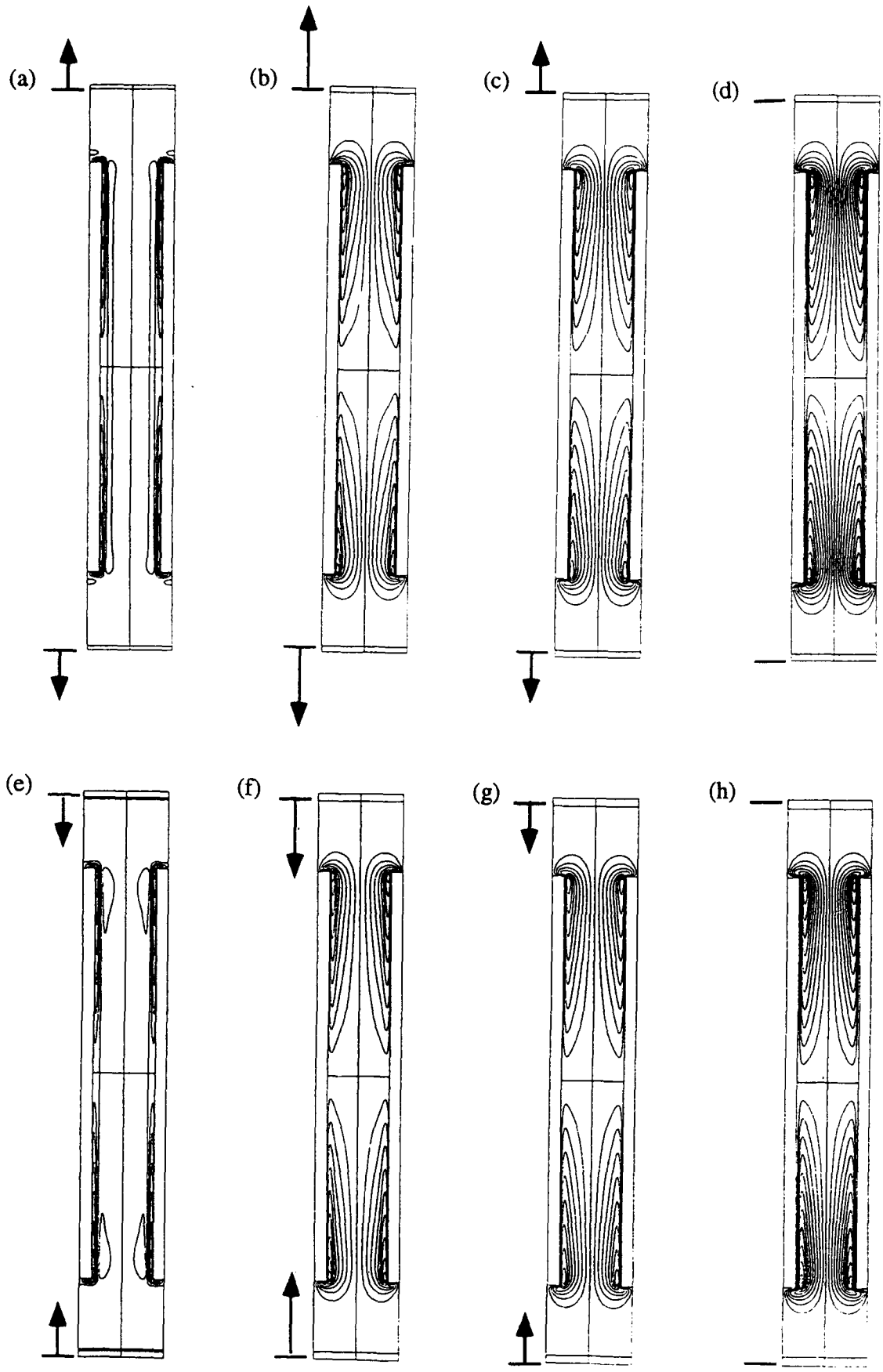

FIG 6: Instantaneous streamfunction distribution in the neighbourhood of a thermoacoustic stack at (a) $\theta = 19.634$,(b) $\theta = 20.42$, (c) $\theta = 21.205$, (d) $\theta = 21.99$, (e) $\theta = 22.77$, (f) $\theta = 23.56$, (g) $\theta = 24.34$, (h) $\theta = 25.132$. The stack has the same dimensions as stack no 1. as used by Atchley [6], (L/H = 4.727 h/H=0.727) and is located at $\tilde{k}\tilde{x}=\pi$. The drive ratio R= 0.13% ; $Re_a = 0.8879$ $Re_p = 0.0096$; $Re_{\dot{o}} = 2132$. The arrows indicate the magnitude and the direction of the acoustic velocity at the matching surfaces.

OFFICE OF NAVAL RESEARCH
PUBLICATION/PATENTS/PRESENTATION/HONORS REPORT
for
1 Oct 93 through 30 Sept 94

R&T Number: TA3126971

Contract/Grant Number: N0001494J0063

Contract/Grant Title: Thermo-fluid mechanic study of thermoacoustic devices

Principal Investigator: A. Prosperetti, C. Herman, and O.M. Knio

Mailing Address: Department of Mechanical Engineering, The Johns Hopkins University, Room 122, Latrobe Hall, 34 N Charles Street, Baltimore, MD 21218

Phone Number (with Area Code): (410) 516-8534; (410) 516-4467; (410) 516-7736

E-Mail Address: prosper@polaris.me.jhu.edu

a. Number of Papers Submitted to Referred Journal but not yet published: 0

b. Number of Papers Published in Referred Journals: 0
(list attached)

c. Number of Books or Chapters Submitted but not yet Published: 0

d. Number of Books or Chapters Published: 0
(list attached)

e. Number of Printed Technical Report & Non-Referred Papers: 0
(list attached)

f. Number of Patents Filed: 0

g. Number of Patents Granted: 0
(list attached)

h. Number of Invited Presentations at Workshops or Prof. Society Meetings: 0

i. Number of Presentation at Workshop or Prof. Society Meetings: 0

j. Honors/Awards/Prizes for Contract/Grant Employees: Charles A. Miller Jr. chair to A. Prosperetti
(list atteched, this might Include Scientific Soc. Awards/Offices, Promotions, Faculty Award/Offices etc.)

k. Total number of Graduate Students and Post-Docs Supported at least 25%, this year on this contract,grant:

Grad Students 2 and Post Docs ____

How many of each are females or minorities? (These 6 numbers are for ONR's EEO/Minority Reports; minorities Include Blacks, Aleuts Amindians, etc and those of Hispanic or Asian extraction/nationality. This Asians are singled out to facilitate meeting the varying report semantics re "under-represented")

- Grad Student Female ____
- Grad Student Minority ____
- Grad Student Asian e/n 2
- Post-Doc Female ____
- Post-Doc Minority ____
- Post-Doc Asian e/n ____